UNIVERSITY OF OKLAHOMA

GRADUATE COLLEGE

MIXTURE OF BIOSURFACTANTS MADE FROM RENEWABLE RESOURCES: SURFACTANT PHYSIOCHEMICAL PROPERTIES

A DISSERTATION

SUBMITTED TO THE GRADUATE FACULTY

in partial fulfillment of the requirements for the

Degree of

DOCTOR OF PHILOSOPHY

By

LOUIS PAUL JACKSON
Norman, Oklahoma
2013

MIXTURE OF BIOSURFACTANTS MADE FROM
RENEWABLE RESOURCES:
SURFACTANT PHYSIOCHEMICAL PROPERTIES

A DISSERTATION APPROVED FOR THE
DEPARTMENT OF BIOENGINEERING

BY

_____
Dr. Brian Grady, Chair

_____
Dr. Matthias Nollert, Co-chair

_____
Dr. Edgar O'Rear

_____
Dr. David Schmidtke

_____
Dr. Ronald Halterman

Acknowledgements

I would like to express the deepest appreciation to my committee chair Professor Dr. Brian Grady, who continually and convincingly conveyed a spirit of excellence in regards to research and scholarship. Without his guidance and persistent help this dissertation would not have been possible.

I would like to thank my committee members, Dr. Matthias Nollert, Dr. Edgar O'Rear, Dr. David Schmidtke and Dr. Ronald Halterman, for supporting me through my academic endeavourers with their insightful expertise of engineering and chemistry.

In addition, a thank you to Professor Dr. Dough Gaffin, whose enthusiasm for teaching and mentoring has had lasting effect. I am in great appreciation to the University of Oklahoma, as it has provided an environment that has allowed me to achieve a monumental milestone not only in my life but in the lives of my family. I also thank my graduate committee and fellow members of the Grady research group whose collaboration increased the quality of Chapters 3 and 4 of my dissertation, which was originally published in the Journal of Surfactants and Detergents.

Table of Contents

List of Tables

List of Figures

List of Figures

Abstract

Complete removal and substitution of non-renewable with renewable surfactants in consumer products is often not possible without the reduction of desirable properties (solubility, wetting, detergency, etc.). The synergetic relationship in mixtures might prove advantageous in reducing the environmental footprint and increasing the biocompatibility of consumer products that use surfactants. Binary aqueous mixtures of (1) alkyl glucopyranosides (glycosides), (2) alkyl maltopyranosides (maltosides), or (3) alkyl *N*-methyl glucamines with (1') sodium alkyl sulfates or (2') sodium *n*-alkyl carboxylates were investigated in an effort to evaluate physiochemical properties for mixtures of surfactants from renewable resources. Through surface tension and nuclear magnetic resonance (NMR) experiments solutions at various concentrations and mixture ratios were evaluated to determine critical micelle concentrations (CMCs). The greatest reduction in CMC was found for surfactants with long and intermediate hydrophobe lengths. In agreement with other studies, an increase in hydrophilic group size and flexibility decreased the electrostatic repulsion of ionic-nonionic mixed micelles as evidenced by a more negative Rubingh's β parameter. However, at low hydrophobe length, carboxylate and glycoside headgroup mixtures produced mixed micelle interactions displaying synergism at low nonionic surfactant mole fractions and slight antagonism at high nonionic mole fractions. The asymmetry in interaction

produces an S-shaped CMC curve and demonstrates that the one-parameter Rubingh model is insufficient in describing both synergism and antagonism for this binary mixture. The analysis of NMR data revealed a stepwise mechanism of micelle formation for 1:9 sodium sodium alkyl sulfates and alkyl glucopyranosides mixtures.

In addition, aqueous solutions of sodium *n*-alkyl carboxylates sodium tetradecanoate (S14C) and sodium dodecanoate (S12C) were used to evaluate complicated precipitation zones and to monitor the effects of bulk pH adjustments on surface tension and CMC determination from surface tension plots. Issues with solubilities of pure sodium n-alkyl carboxylates in solution near the critical micelle concentration (CMC) have been reported previously many times. In this study, some solubility issues encountered with solutions prepared from vendor-supplied S12C were resolved through additional purification. As sodium alkyl carboxylates presented in the literature are commonly used as received from the manufacture without additional purification, the wide range of reported CMC values as well as solubility issues for S12C are likely due to impurities as well. However, solubility for S14C solution concentrations near reported CMC values were not resolved through additional purification of purchased material. We believe that CMC values reported in the literature for C14S should be reconsidered, as breaks in surface tension relationships are likely caused by the formation of precipitate not

micelle aggregation. In addition and in agreement with other studies, solution pH adjustments revealed an optimum surface tension for maximum solubility near S14C pK_a values.

Chapter I

Surfactant Background

1.1 Structural and Chemical Properties

Surfactants are organic compounds possessing both hydrophobic and hydrophilic motieties. Figure 1.1 displays the schematic representation of a surfactant. These amphiphilic molecules are surface active agents that reduce interfacial tensions.

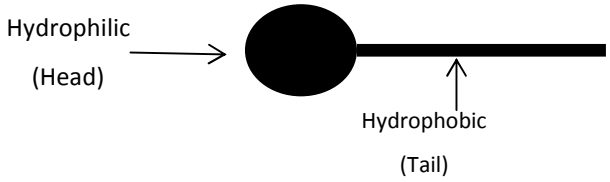

Figure 1.1 Schematic representation of surfactant.

Dissolved in water, surfactants hydrophobic groups distort the structure of water and therefore increase the free energy of the system. To minimize free energy, at low concentrations surfactant molecules concentrate at the surface, orienting hydrophobic groups away from the solvent. At higher concentrations when the surface nears surfactant saturation, surface-active molecules aggregate with their hydrophobic groups directed towards the interior resulting in micelle formation [1]. Micelle formation is an important phenomenon in interfacial interactions such as detergency and solubilization [2]. Figure 1.2 provides a schematic of the processes described above.

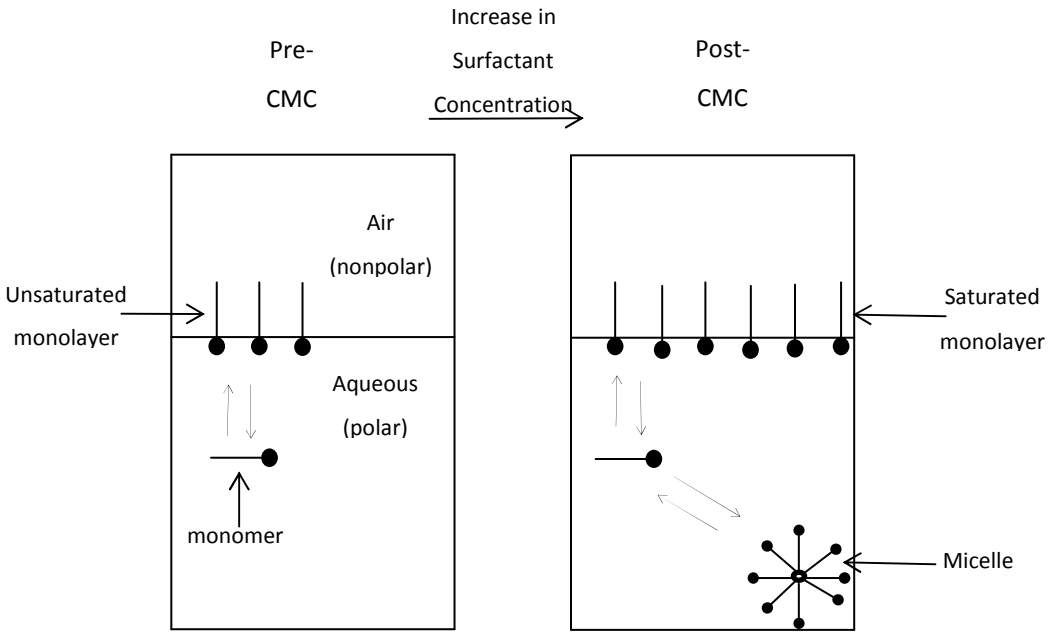

Figure 1.2 Schematic of surfactant behavior in aqueous solution.

Due to their simple intrinsic properties and chemical versatility surfactants have been heavily utilized in the following consumer products: detergents, cleaning products, cosmetics, facial cleaners, shaving creams and deodorants [3-5].

1.2 Commercial Applications

Initially utilized as a cosmetic hair pomade by the Gauls more than 3000 years ago [6], it has only been within the last 1000 years that surfactants have been used as a general purpose cleaner. Multicomponent systems were first introduced by Germany in the 20th century and were used as laundry detergents and were "self-acting" for routine washing of textiles. Improvements and selective enhancements of multicomponent systems were further achieved with the introduction of synthetic surfactants and was generally accepted worldwide with the introduction of Tide by Proter & Gamble in 1946 [7]. However, due to

the low biodegradability and environmental toxicity caused by branched tetrapropylenebenzenesulfonate (TPS) containing formulations of the 1950, replacement with more rapidly and effectively degradable linear alkylbenzenesulfonates, nonylphenol ethoxylates, alkyl sulfates and sodium alkyl carboxylates have been promoted socially and enforced legally [7].

Recently an increased interest and use of surfactants made from renewable resources has arisen in order to give commercial surfactants a favorable environmental “green” image. Biosurfactants are surface active molecules that contain head and tail groups produced by a variety of microorganisms mainly bacteria, fungi and yeast. The renewable headgroup components can also be chemically tethered to petroleum based linear hydrocarbon tails or renewable linear hydrocarbon constituents produced from locally available resources (ie. grasses and wheat). Biosurfactants are often prepared under harsh chemical conditions with the use of environmentally unfriendly polar solvents [8, 9]. An exception is the manufacture of alkyl polyglucosides (APGs) which are produced under mild reaction conditions. To further reduce environmental hazards and decrease the carbon footprint made by biosurfactants the use of enzymes in surfactant manufacturing has increased [17].

As displayed in figure 1.3 surfactants are commonly classified into four categories based on the formal charge presented in their lyophobic headgroup

and are as followed: anionic (negatively charged), cationic (positively charged), nonionic (uncharged) and amphoteric (zwitterions containing both positive and negative charges at defined pH).

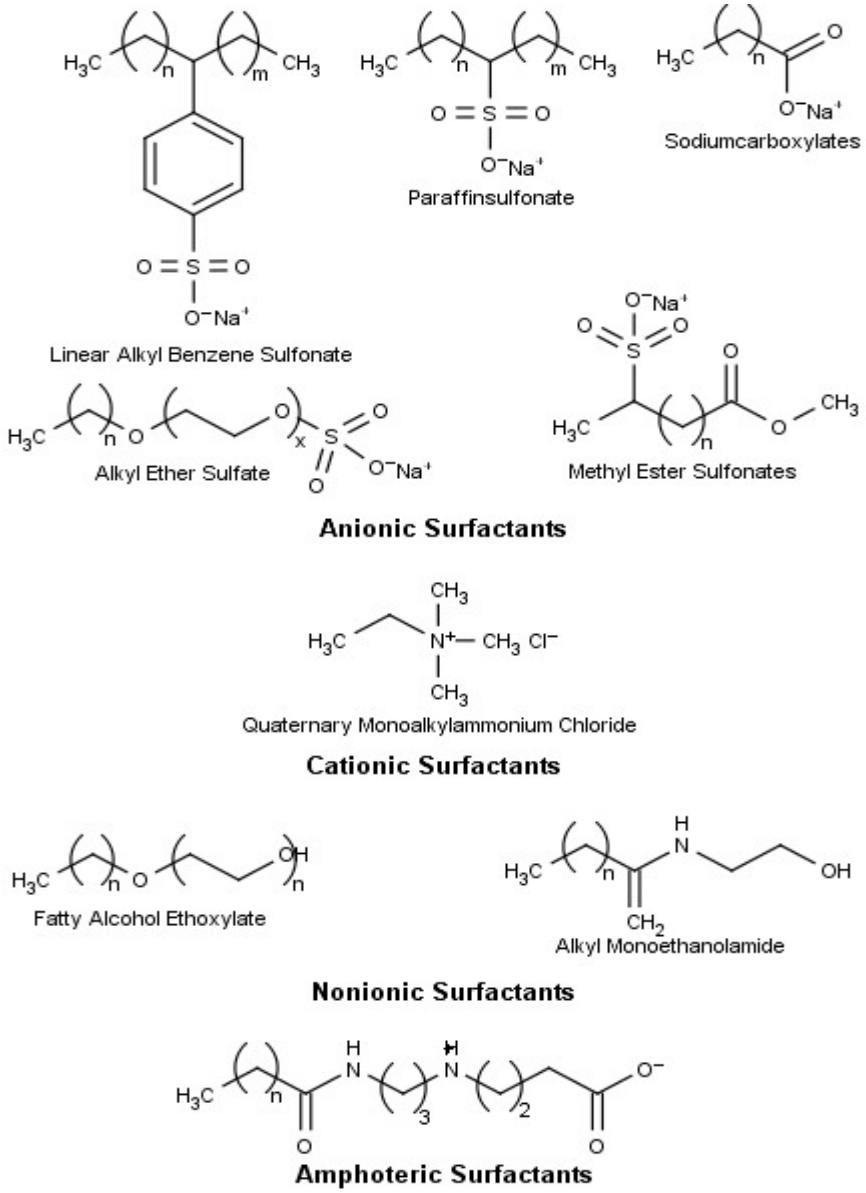

Figure 1.3 Common surfactants used in consumer formulations.

Modern consumer formulations are comprised of 20 or more ingredients depending on what benefits the product is meant to provide [6]. For the household industry, the most common anionic surfactants are those with a sulfate, sulfonate, or carboxylate headgroup [10]. Anionic salts are sensitive to low pH and electrolytes in solution, producing water-insoluble fatty acids. As precipitation generally renders the surfactant ineffective in solution, the task of effectively and efficiently combining additives for ideal performance has proven quit difficult due to the complexity of the cleaning process and the large variations in particulate matter and substrate.

For optimum product performance it is important to understand and describe molecular and bulk interactions of surfactants in solution such as micelle formation [11, 12], adsorption at interfaces [13], wetting [14], emulsification [15], detergency [7], foaming and antifoaming [16]. However, to date we do not have the ability to completely and accurately describe all the interactions presented above. To minimize molecular and bulk interactions experienced in real world product applications, a bottom-up approach is used in this study to evaluate pure surfactants in solution and binary mixed surfactant systems. The study will present surface tension and nuclear magnetic resonance (NMR) spectroscopy experimental data used to determine critical micelle formation (CMC) for pure and binary (anionic-nonionic) surfactant systems, as well as the mixing behavior according to Rubingh's one parameter model for

selected binary systems. In addition surface tension plots of selected sodium n-alkyl carboxylate are collected and used to evaluate complicated precipitation zones. The presented studies will ultimately assist in improvement of current theoretical tools or the development of novel theoretical tools needed for the optimal selection and evaluation of amphiphilic molecules used in scientific, commercial and industrial research and development.

Chapter II

Experimental

2.1 Materials

The following alkyl sulfates and sodium alkyl carboxylates were purchased from Sigma Aldrich (St. Louis, MO, USA): sodium dodecyl sulfate (S12S), sodium decyl sulfate (S10S), sodium tetradecanoate (S14C), sodium dodecanoate (S12C) and decanoic acid (S10H). The sodium surfactant salt sodium decanoate (S10C) was prepared by neutralizing the corresponding acid from Sigma Aldrich with an equimolar quantity of sodium hydroxide. After refluxing for 2 hr in a 3:1 ethanol/water solution, the salt was crystallized from cooled solution to 4°C, washed with anhydrous acetone, and dried under vacuum. Nonyl-, octyl- and heptyl-glucopyranoside (GPN#, where #=9, 8, 7 respectively), nonyl- and octyl-β-D-maltopyranoside (2GPN#, where #=9,8 respectively), as well as decyl-, nonyl-, and octyl-*N*-methylglucamine (MEGA#, where #=10, 9, 8 respectively), were purchased from Anatrace (Affymetrix-Santa Clara, CA, USA). All surfactants were received at greater than 99% purity and used as received without further purification for experiments conducted in Chapter III.

The S14C and S12C used in Chapter IV were received at greater than 99% purity and further purified through recrystallization techniques. Vendor-

supplied surfactant powders were dissolved in a 4:6 ethanol and water solvent solution at 60˚C. The solute was allowed to slowly cool to room temperature and then filtered through #1 Whatman® filter paper using a Buchner funnel and suction. The isolated and purified powders were washed with cool 4:6 ethanol and water solution, and vacuum dried. The S12C and S14C materials were recrystallized in this manner three times prior to use. Glassware used in this study was cleaned using Nochromix^{TM}. Molecular structures of surfactants used in this study are shown in Figure 2.1.

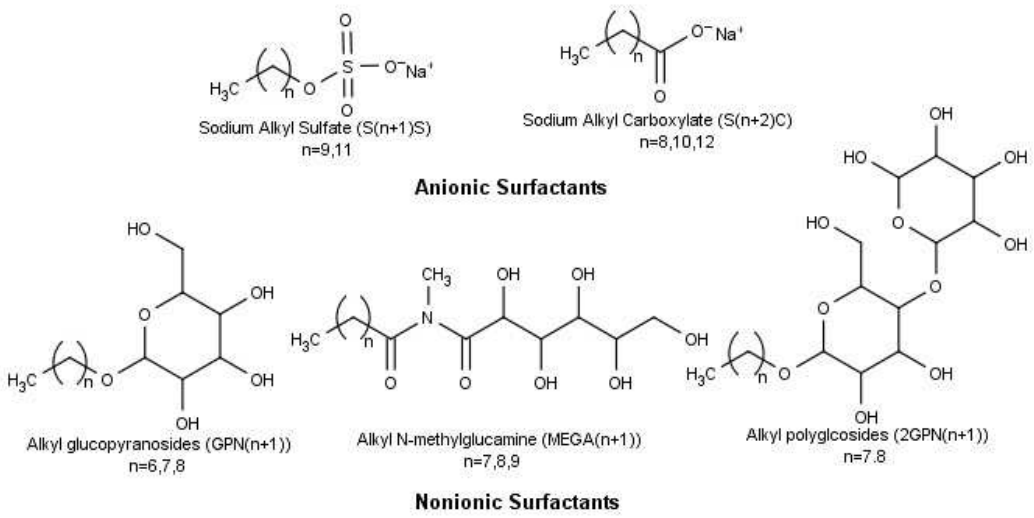

Figure 2.1 Molecular structures of anionic and nonionic surfactants.

2.2 Methods

All solutions in chapter III were evaluated at a pH 8.0 (except where specified) in 18 MΩ deionized water using freshly prepared solutions at 25°C. Pure S12C and S14C experiments were carried out at two adjusted pH regimes of 7.2-7.5 and 10.5 with all other experimental conditions as stated above. pH adjustments were made via sulfuric acid (H_2SO_4) or sodium hydroxide (NaOH). Different pH's were required because of insolubility of vendor supplied S12C and S14C at concentrations near the CMC at 25°C and a pH 8.0. Solution pH adjustments in chapter IV were made for every surfactant concentration evaluated in part of the experimentation; in some cases the pH was not adjusted. pH was adjusted via sulfuric acid (H_2SO_4) and/or sodium hydroxide (NaOH) and monitored with an Oakton (PC 100) pH meter (Veron Hills, IL, USA).

A Wilhelmy Plate method with a silica plate probe was used to determine surface tension (γ). In this method, the plate is oriented perpendicular to the interface and the force excreted on it is measured as displayed in Figure 2.2.

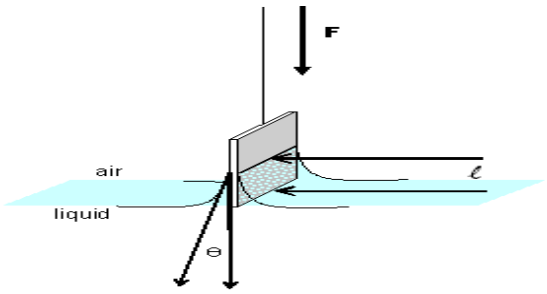

Figure 2.2 Illustration of Wilhelmy Plate method with a silica plate probe

The surface tension for all solutions were determined as described in equation

$$\gamma = \frac{F}{l \cdot \cos\Theta} \qquad 2.1$$

where is the wetted perimeter of the plate, F is the force of gravity and Θ is the contact angle between the liquid phase and plate. Data in Figure 2.3 is a representative example of data obtained from the Cahn DCA and was analyzed to determine CMC, surface tension at CMC and surface tension reduction efficiency (pC_{20}) as shown on the figure.

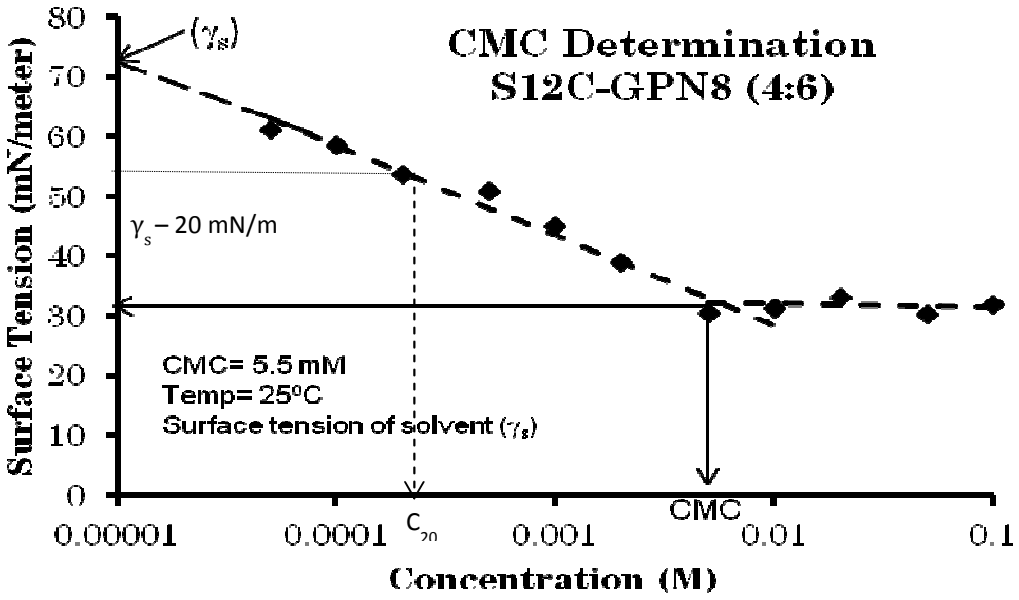

Figure 2.3 Representative surface tension - log C plot to show how (CMC) and (pC_{20}) were determined which shows the data quality for these experiments. Dashed lines are fits to data based on a least squares criterion, where diamonds are data.

All CMC values were determined through linear regression fits done using Excel Solver. There are two linear relationships observed in the surface tension - log C plots, one below and one above the CMC. The concentration region below the CMC is described by the Gibbs Isotherm [1], which is the region where added surfactant still lowers the surface tension. To find the CMC first Excel Solver was used to determine the linear regression fit from experimental data collected in the Gibbs Isotherm region. A second linear regression fit was then resolved for data points collected at concentrations above the Gibbs Isotherm. The intersection of the two independent lines was then solved to determine the CMC of the given solution.

The selection of surfactant concentration regimes for regions within and above the Gibbs Isotherm was not trivial. In this study surfactant concentration selection was based on visual preference which unavoidably introduced bias. However, the effect of selection bias in this study was shown to be limited as CMC data from each hydophobe grouping low, intermediate and high was found to have a standard deviation of $\pm$0.03,$\pm$0.12 and $\pm$0.2 respectively when averaging 3 visually selected fits. For future CMC determination it is suggest that if a CMC change greater than 20% is observed when using averaging criteria presented above, rejection or reconsideration of observed fits should be considered.

All non-linear regression fits of CMC data to determine β were done using Excel Solver and an original Visual Basic program. Equations 3.2 and 3.3 require micellar compositions, which were also fitted. An iterative routine was used, where first the micellar composition (X), and then the beta parameter were fit. To determine the former, Equations 3.2 and 3.3 were used independently to calculate CMC_{12} and the least squares difference between the two CMC_{12} was minimized. Then, β was fit to minimize the least square difference between the average calculated CMC_{12} values from the first iteration and the measured CMC_{12} values. The number of iterations was determined when the fitted beta parameter did not change by more than one part in a thousand. For determination of χ^2, the relative standard deviations were assumed to be identical for all samples and were calculated by averaging values for 4 samples that were repeated at least three times each. Dashed lines in Figures 3.1-3.4 correspond to +/- 10% variation to the fitted beta parameter. Surface tensions were measured with a CAHN 322 DCA (Madison, WI, USA) which is displayed in Figure 2.4.

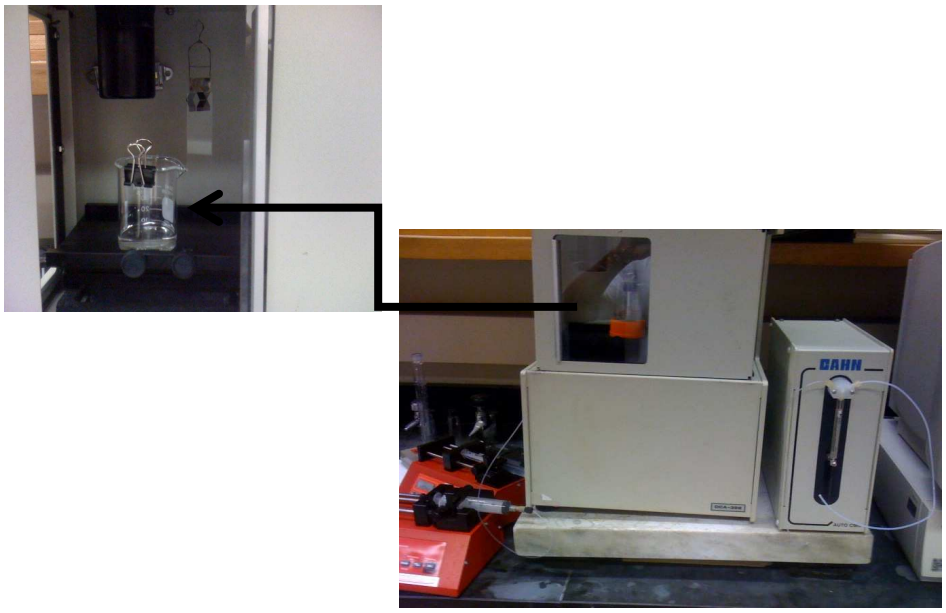

Figure 2.4 CAHN DCA-322

Chapter III

Mixtures of Nonionic Surfactants with Alkyl Sulfates and Sodium n-Alkanecarboxylates: Comparison of Mixing Behavior using Rubingh's Treatment

3.1Introduction

Due to the increasing consumption of non-renewable petroleum based products and the high price of oil, a growing demand for "green" surfactants, that is surfactants from renewable resources, has arisen. Criteria for the use of surfactants from renewable resources in consumer products such as shampoos, toothpaste, etc. consist of low CMC, fast wetting kinetics, high biodegradability, and an ability to be produced in large volumes [10]. However, these properties are limited due to the significant synthetic chemistry constraints placed on renewable surfactant production. Alkyl *N*-methyl glucamines (MEGA) and alkyl glucopyranosides (glycosides/GPN) are two renewable nonionic sugar-based surfactants synthesized from locally produced raw materials.

Molecularly similar sugar-based alkyl maltoside polyglycosides (2GPN) have been found to be both highly biodegradable and have low toxicity [17, 18]. However, nonionic surfactants are often not included in consumer products as primary surfactants due to low foaming capacity, less stable foam, and hardness of their detergency [10]. Instead, in many consumer products, nonionic

surfactants are mixed with ionic surfactants, most commonly anionic surfactants. Though anionic salts are used as the primary surfactant in many consumer formulations, toxicology studies have shown that concentrations of sodium alkyl sulfates as low as 0.5% could cause irritation and concentrations of 10-30% cause skin corrosion and severe irritation [1]. In addition, increased aphthous ulcer formation caused by surfactants like sodium lauryl sulfate contained in toothpaste have been reported [2, 3].

Anionic sodium n-alkyl carboxylates have show to be less irritating and have equivalent physical properties (at a more narrow concentration regime then sodium lauryl sulfate), but due to low hardness tolerance (i.e. resistance to precipitation induced by calcium or magnesium ions) and solubility issues caused by pH sensitivity they have been used in consumer formulations in a lesser extent then sodium lauryl sulfates. Due to increased reports of adverse effects (skin irritation, skin corrosion and/or aphthous ulcer formation) caused by anionic surfactants, formulations containing highly biocompatible surfactants with low toxicity like nonionic alkyl glycosides and maltosides, as well as the broader molecular weight distribution analogues polyglucosides, will be in higher demand.

Synergism in surfactant mixtures has been observed in anionic-cationic, anionic-nonionic, cationic-nonionic, and even nonionic-nonionic mixtures [19]. In this study, alkyl sulfates and sodium *n*-alkyl carboxylates are used as anionic

surfactants in mixtures with nonionic MEGA, GPN and 2GPN surfactants. The anionic surfactants are made from either natural or petroleum feedstocks, while the hardness tolerance (i.e. resistance to precipitation induced by calcium or magnesium ions) for these surfactants is quite low. Pure anionic surfactants have significant electrostatic self-repulsion while pure nonionic surfactants have weak steric self-repulsion and both reduce the driving force to form micelles [2].

However, after mixing, the electrostatic self-repulsion of the ionic component is reduced by shielding from the nonionic headgroups in the mixed micelle at low nonionic concentration. When nonionic surfactants are the major constituent in mixed micelles, the smaller anionic headgroups reduce steric self-repulsion of the nonionic headgroups. Self-repulsion for nonionic surfactants is caused by steric interactions of its bulky hydrophilic or hydrophobic headgroups [20]. In addition van der Waals interaction between hydrophobic groups [21], and possible hydrogen bonding between hydrogen acceptor and donor groups[22] limit the degrees of freedom of the surfactant aggregates increasing self-repulsion.

Specific surfactant pairing was based on CMC-matching, i.e. a particular anionic surfactant was paired with a particular nonionic surfactant based on the criterion that the CMCs of the pure materials were approximately equivalent. This type of matching allows symmetric evaluation of synergism within the system; i.e. the CMC vs. mole fraction curve is approximately symmetric. The

relative reduction in CMC vs. the lowest pure CMC component of the binary system under investigation is also more pronounced in systems where the CMCs are matched. A low, medium and high grouping was defined with pure CMCs of approximately 10, 20 and 75 mM respectively. Molecular or hydrophobe size could have been equally valid in terms of a selection criterion; however, symmetry of the CMC curve would not be possible as, for these surfactants, matching either of these criteria would not have led to roughly equivalent CMCs.

From a previous study by our group [23], promising properties and interactions (lower CMC) have been observed in mixtures of nonionic renewable surfactants with non-renewable anionic alkyl sulfates. Due to the expected growing importance and demand of highly biocompatible nonionic surfactants from renewable resources and the importance of anionic/nonionic mixtures commercially, we have continued our investigations of these mixtures with respect to their ideality of mixing according to Rubingh's one parameter model for the CMC.

3.2 Theoretical Background

Theoretical understanding of the mixing behavior of mixed surfactant systems was first described by the pseudophase separation model, which treated micelles as a separate phase with ideal (i.e. entropic only) mixing of the binary system [27, 28]. The pseudophase separation model does not predict or fit data

to synergetic or antagonistic behaviors, but relates the chemical potential to determine the CMC of the mixed surfactant system under investigation [29]:

$$CMC_{12} = \left[\left(\frac{\alpha}{CMC_1}\right) + \frac{(1-\alpha)}{CMC_2}\right]^{-1} \qquad 3.1$$

where α is the total mole fraction of surfactant 1 (includes surfactant 1 in solution and in micelles), $CMC_{12,}$ CMC_1, and CMC_2 are the critical micelle concentrations of the mixed surfactant, pure surfactant 1 and pure surfactant 2 respectively. Though this approach has proven successful when describing surfactant mixtures of similar molecular properties and structure, molecularly dissimilar surfactant mixtures deviate from ideal mixing.

To account for non-ideal mixing, Rubingh's treatement used in this study builds upon the pseudophase separation model by introducing the interaction parameter β [30]. If β= 0 an ideal solution is assumed and surfactant behavior follows regular solution theory and indicates pure entropically-driven mixing. A negative β parameter indicates mixing that is more alternating than random; i.e. the two different surfactants would rather be next to each instead of being located next to a similar surfactant. With X defined as the mole fraction of surfactant one in mixed micelles, the CMC of the binary solution (CMC_{12}) is shown in the following two equations [16]:

$$CMC_{12} = \frac{\{\alpha CMC_1 + \exp[\beta(1-X)^2]\}}{\alpha} \qquad 3.2$$

$$CMC_{12} = \frac{\{(1-X)CMC_2 \exp[\beta X^2]\}}{(1-\alpha)} \qquad 3.3$$

The conditions for synergy to exist can be determined by independently solving Equations (1) or (2) with the conditions that $CMC_1 < CMC_2$ and that $dCMC_{12}/d\alpha = 0$ at a point of maximum synergism. The conditions for synergy to exist are [20] :

1. β must be negative
2. □ ln (CMC_1/CMC_2)□ < □β□

If the individual CMCs of the two surfactants in solution are similar (i.e. ln (CMC_1/CMC_2) ~ 0), any negative β parameter will represent synergism, and β will represent a reduction in CMC and favorable interaction between surfactant. Adjustments of this interaction parameter have produced well defined fits with experimental CMC data in many previous studies [31, 32]. β values can be explained qualitatively when comparing the chemical potential of pure A or B surfactant solution to the chemical potential of a AB mixture. When β =0 the chemical potential of pure A or B is equal that of an AB mixture. However, a positive or negative β values represents an increase or decrease respectively in chemical potential of the mixed system relative to the pure systems.

Other more complicated model such as Maeda [33] or Puvvada and Blanckschtein [34] could be applied to the micelle composition. However, such models have no inherent advantage over that of Rubigh.

3.3Results and Discussion

Table 3.1 shows the CMCs found in this study for all pure surfactants as well as various values measured in the literature. S14C and S12C were partially insoluble at pH 8.0; solubility was restored by adjusting pH of the surfactant solutions. We found pH and solubility regimes for specific S12C and S14C concentrations; solubility occurred for a small pH of (7.1-7.5) as well as at pH 10.5 for all concentrations (0.01-100 mM) evaluated. At pH 7.1-7.5 the CMC for S14C and S12C was evaluated to be 3.2 and 16.3 mM respectively, while for pH 10.5 CMCs were 5.5 and 22.1 respectively. Values reported in Table 3.1 and used in least square fittings for S14C and S12C were determined from interpolated values at pH 8.0 as 4.0 and 17.3 respectively. For mixtures of anionic and nonionic surfactants, no anionic surfactant insolubility was found at pH 8.0 likely because the concentration of monomeric surfactant was lowered due to the formation of mixed micelles.

Although this topic will be fully explored in chapter IV, it is important to note that a number of authors have also reported issues with the solubility of pure S12C and S14C solutions. Lucassen [20] and Kralchevska et al. [21]

previously described the degree of pH sensitivity and different zones of precipitation for sodium n-alkyl carboxylates solutions that result in the formation of neutral-soap, acid-soap and alkanoic acid crystallites. For S12C and S14C, an increased concentration and dissolution in water is accompanied by an increase in pH due to protonation (hydrolysis) of the oxygen connected to the carbonyl leading to turbidity of the soap solution [35]. We also observed a depression in surface tension as a result of increased H_2SO_4 or NaOH concentrations , a trend also described in the literature [36, 37]. The wide range of CMC values for S12C presented in the literature is likely related to the lack of control of surfactant purity (see Table 3.1).

Table 3.1 Chemical name, abbreviation, molecular formula, molecular weight, CMCs from literature and CMCs measured from this study. The triple lines separate the table into low, medium and high CMC values.

Chemical[1] Name	Abbr.	Molecular Formula	Molecular Weight	CMC from[3-9] Literature (mM)	CMC found[2] in this study (mM)
Sodium Dodecyl Sulfate	S12S	$C_{12}H_{25}SO_4Na$	288.33	7.9^{ST} ,8.0^{EPR}(20°C), 8.2^{ST},8.4^{MP} [38-41]	7.7
Sodium Tetradecanoate	S14C	$C_{14}H_{27}NaO_2$	250.35	4.0^{C},$6.9^{ST,C}$, [42, 43]	4.0
n-Nonyl-*β*-D-Glucopyranoside	GPN9	$C_{15}H_{30}O_6$	306.4	6.5^{NMR} [44]	6.2
n-Nonyl-*β*-D-Maltopyranoside	2GPN9	$C_{21}H_{40}O_{11}$	468.5	6.0 [45]	8.2
Decanoyl-*N*-Methylglucamide	MEGA10	$C_{17}H_{35}NO_6$	349	5.0^{F},4.8^{F},7.0^{P} [46-48]	7.1
Sodium Decyl Sulfate	S10S	$C_{10}H_{24}SO_2Na$	260.33	26.9^{C} [45]	21.3
Sodium Dodecanoate	S12C	$C_{12}H_{23}NaO_2$	222.3	14.3^{ST} (20°C),9.9^{ST}(30°) 28.6^{C}(20°C),26.1^{C} (30°C) 23.0^{ST},25.7^{C},28.1^{C} [43, 49-52]	17.3
n-Octyl-*β*-D-Glucopyranoside	GPN8	$C_{14}H_{28}O_6$	292.4	23.2^{NMR} 26.0^{ST}(22°C),24.5^{F} [44, 53, 54]	19.4
n-Octyl-*β*-D-Maltopyranoside	2GPN8	$C_{20}H_{38}O_{11}$	454.4	19.5 [45]	24.9
n-Nonanoyl-*N*-methylglucamide	MEGA9	$C_{16}H_{33}NO_6$	335.5	16.0^{F},25.0^{P} [47, 48]	18.7
Sodium Decanoate	S10C	$C_{12}H_{19}O_2Na$	194.25	85.0^{C}, $95.5^{ST}$$106.0^{C}$, 116(20°C)^{NMR} [43, 55-57]	77.6
Heptyl-*β*-D-Glucopyranoside	7GPN	$C_{13}H_{26}O_6$	278.4	70.0^{C} [45]	80.0
Octanoyl-*N*-Methylglucamide	MEGA8	$C_{15}H_{31}NO_6$	321.4	51.3^{F},54.8^{ST} [47, 58]	32.4

1. Molecular structures of the compounds in the Table are provided in Fig. 1.
2. All literature CMC values reported were collected at 25°C and pH 8.0,unless otherwise stated.
3. STCMC was obtained by Surface Tension data.
4. ^{C}CMC was obtained by Electrical Conductivity data.
5. ^{F}CMC was obtained by fluorescence.
6. ^{P}CMC was obtained by photometric assay.
7. ^{NMR}CMC was obtained by chemical shift coefficients of methyl group protons.
8. ^{EPR}CMC was obtained by evaluation of electron paramagnetic resonance
9. ^{MP}CMC was obtained by membrane potential studies.

Data for MEGA8 in Table 3.1 was very different than that of reported literature values. Our value for the CMC of MEGA8 32.4 mM, seems in line with the measured value of MEGA10 and MEGA9. Similar CMC values as reported in this paper were found in a previous study [23] by our group with MEGA8 purchased from the same distributor although the same bottle was not used for this study. Examination of the trend of CMC with increasing chain length shows the addition of one carbon unit to the hydrophobe length tends to reduce the CMC by a factor of 2-3. The underlying thermodynamic process is based on the additional methylene group's ability to add water molecules near the hydrophobic chain, producing an increase in entropy upon release due to transfer of the surfactant from bulk solution to the air-water interface and is often termed the Traube rule [59]. This trend has been well established previously and shown to be valid for several homologous series of anionic, cationic, and nonionic surfactants [60-64].

Table 3.2 display β parameters for all mixtures evaluated in this study. The β parameter indicates the mixing behavior of binary surfactants systems; where a positive or negative β value indicates an antagonistic or synergistic behavior respectively given the fact that the CMCs were approximately identical.

Table 3.2 Effects of hydrophobe length and flexibility of nonionic surfactant on mixed micelle interaction

Anionic-nonionic System	**$\lvert \ln (CMC_1/CMC_2) \rvert$**[1]	**β Parameter**[2]
S12S-GPN9	0.22	-1.9
S12S-2GPN9	0.17	-3.3
S14C-GPN9	0.44	-3.4
S14C-2GPN9	0.72	-4.5
S14C-MEGA10	0.57	-4.0
S10S-GPN8	0.05	-1.8
S10S-2GPN8	0.20	-1.7
S12C-GPN8	0.11	-4.4
S12C-2GPN8	0.36	-5.8
S12C-MEGA9	0.08	-5.0
S10C-GPN7	0.05,0.06	-1.6[3], 0.1[4]
S10C-MEGA8	0.83	-1.7

[1]The condition for synergy to exists as descried by Rosen[10]: □ ln (CMC1/CMC2)□ < □ β □.

[2]β parameters determined as described in Equations 2 and 3.

[3]β parameters of S10C-GPN7 at low (0-0.4) mole fraction of nonionic 7GPN. An accurate fit to Rubingh's treatment over the entire mole fraction range was not appropriate so β parameters for low molar nonionic and high molar nonionic were calculated independently.

[4]β parameters of S10C-GPN7 at high (0.6-1) mole fraction of nonionic 7GPN.

Figures 3.1 and 3.2 show CMCs as a function of mole fraction of nonionic component and least-square fits to the data using Equations 3.2 and 3.3 for sodium n-alkyl sulfate and sodium n-alkyl carboxylates mixed with nonionic GPNn and 2GPNn surfactants respectively. β parameters for the S12S-GPN9 and S10S-GPN8 binary surfactant systems were determined in a previous study by our group [23]; for the S12S-GPN9 and S10S-GPN8 an average fitted beta parameter of -1.9 and -1.8 was found in this study as compared to -1.8 and -1.3 of the previous study. Synergisms between both alkyl sulfates and n-alkyl carboxylate were greatest for the 2GPNn compared to the GPNn binary systems in three out of four group pairings as indicated by more negative β parameters in Figures 3.1-3.3. 2GPNn has a headgroup that is roughly twice the size as that of GPNn head group. Also, 2GPNn has a flexible ether bond between the two rings which provide increased flexibility. We believe the size and increased degree of freedom of the 2GPNn headgroup provides more efficient shielding of sodium alkyl sulfates and sodium alkyl carboxylate headgroups, e.g. a "wrapping mechanism". Support for this proposed mechanism is provided when comparing nonionic headgroups in mixtures of less flexible decyl glycoside/S12S and more flexible decyl maltoside/S12S which produces β parameters of -2.3 and -3.3 respectively [65].

The effect of headgroup size was further described by Joshi et al. [66], observing similar but not as pronounced trends in their magnesium dodecyl

sulfate/C12E12 and magnesium dodecyl sulfate/C12E15 mixtures with β parameters of -1.22 and -1.60 respectively. Zho and Rosen also report β parameters for C12E4 and C12E7 with S12S as -0.84 and -2.34 respectively, concluding that increased length of hydrophilic groups decrease electrostatic self-repulsion in mixed systems, resulting in increased synergism[2]. However, headgroup size and "wrapping" effects seem to be overshadowed by packing constrains resulting from reduced hydrophobe chain length for the shortest hydrophobe chain groupings (S10S-GPN8 and S10S-2GPN8), causing the roughly equivalent β parameters observed in the S10S mixtures displayed in Figure 3.1 c-d.

Though both negatively charged, sodium n-alkyl carboxylate and glycoside mixtures displayed comparatively more negative β parameters than that of the sodium n-alkyl sulfates and glycoside mixtures as displayed when comparing Figure 3.1 and 3.2 This trend was also reported by Prokhorova and Glukhareva; S12S-GPN and S14S-GPN compared to S12C-GPN and S14C-GPN show β parameters of -3.3, -2.5 and -4.1, -3.4 respectively [67]. The n-alkyl sulfate/glycoside mixtures in our study displayed less synergy, i.e. less negative β parameters, compared to values reported by Prokhorova and Glukhareva, and greater synergy in the intermediate hydrophobe sodium n-alkyl carboxylate/glycoside mixtures [32]. Equivalent synergy was observed when comparing the S14C-GPN mixture from the current study to that reported by

Prokhorova and Glukhareva [32]. Our study consisted of pure GPN constituents as compared to the previous study which used commercial glycoside mixtures that contained a mixture of hydrophobe and hydrophile lengths. The charge of a surfactant's headgroup has also been shown to effect micelle formation in ionic-nonionic mixtures containing glycosides. A previous study found that a anionic-nonionic S12S/GPN10 mixture had a β parameter of -2.3 compared to a β parameter of -4.1 for the cationic-nonionic dodecyltrimethylammonium bromide/GPN10 mixture [65].

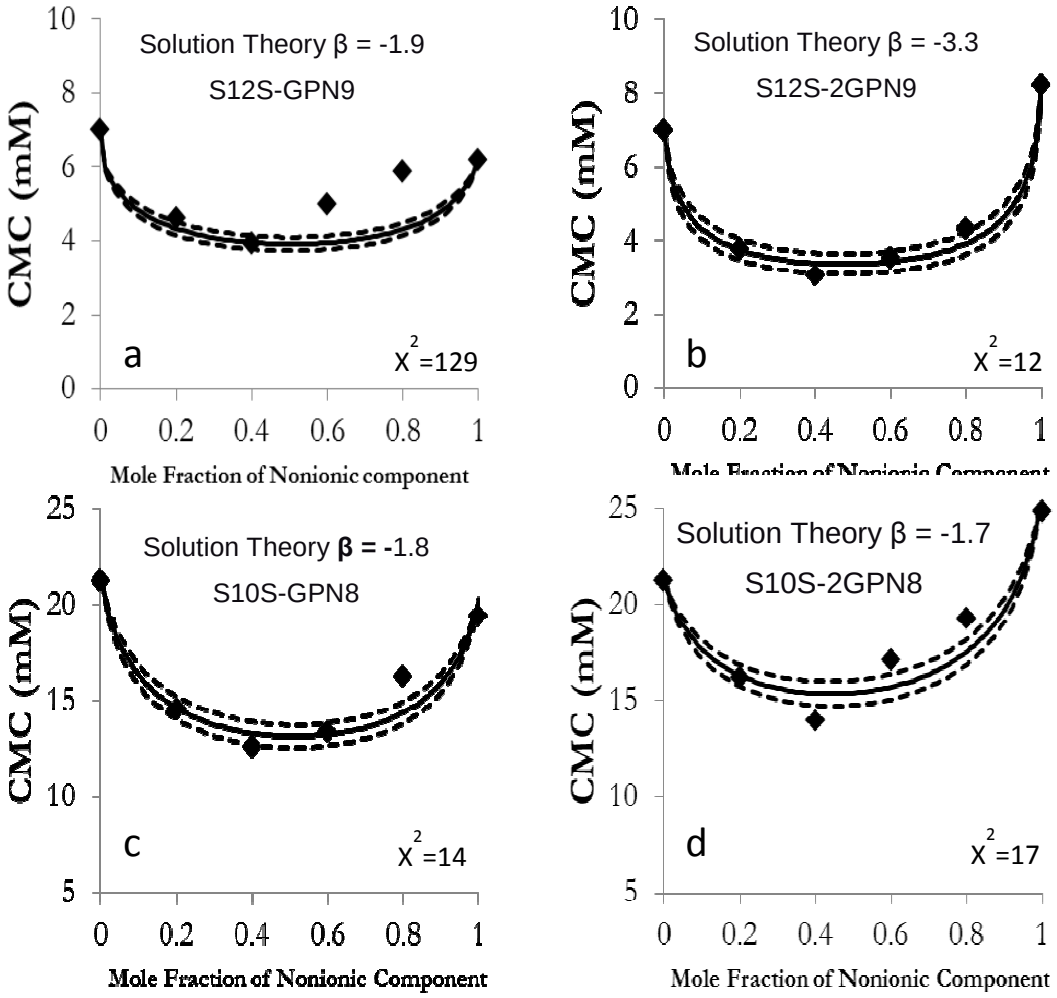

Figure 3.1 Experimental (♦) and predicted (□ □) CMC values for a) S12S-GPN9 b) S12S-2GPN9, c) S10S-GPN8, and d) S10S-2GPN8 as a function of the mole fraction of nonionic component. The solid line is the best fit to the data according to Equations 2 and 3, with dashed lines representing ±10% of the fitted β value.

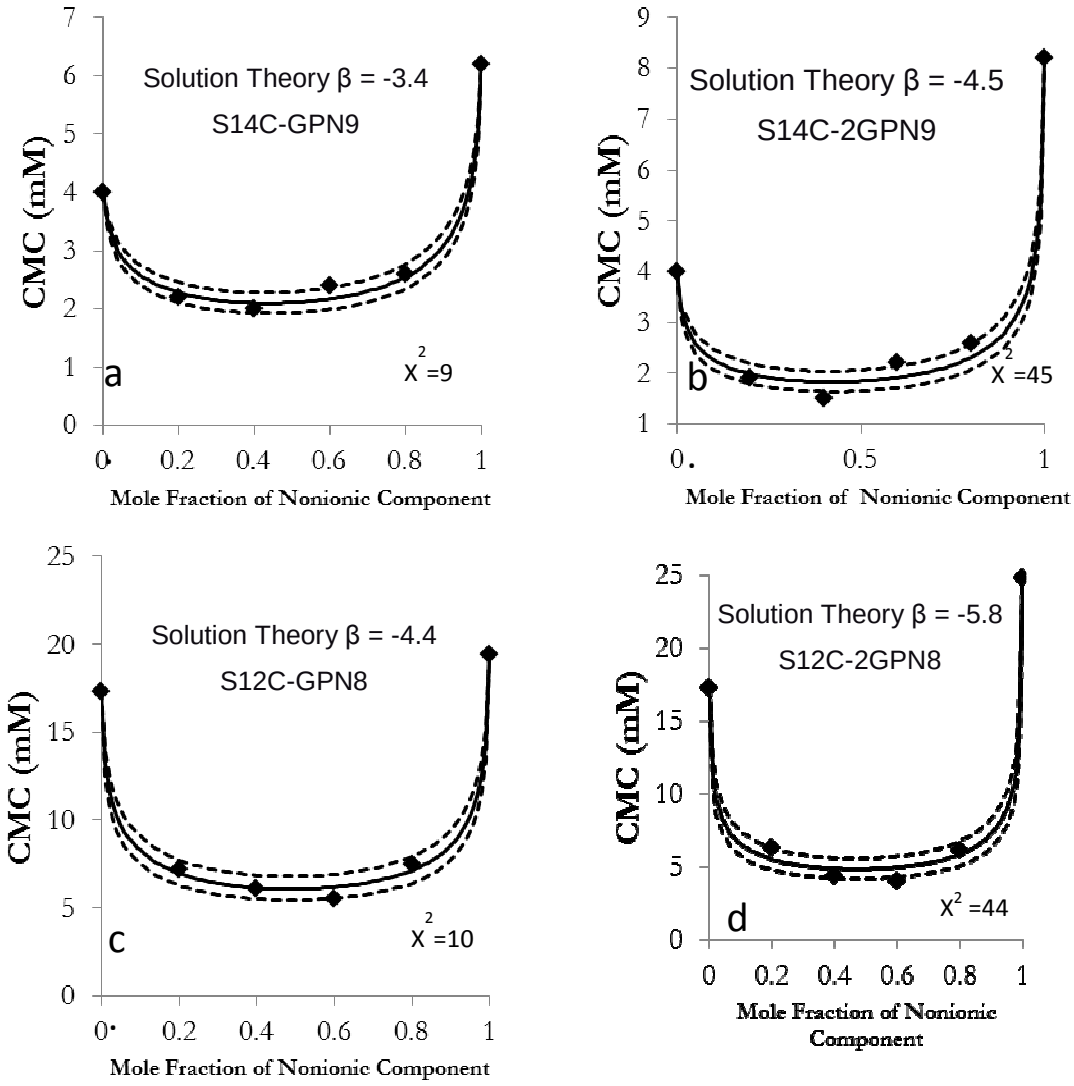

Figure 3.2 Experimental (♦) and predicted (□ □) CMC values for a) S14C-GPN9 b)S14C-2GPN9, c) S12C-GPN8, and d) S12C-2GPN8 as a function of the mole fraction of nonionic component. The solid line is the best fit to the data according to Equations 2 and 3, with dashed lines representing ±10% of the fitted β value.

Figure 3.3 shows CMC data and non-ideal solution theory fit to the data for S10C-GPN7 mixtures. Inspection of the plot in Figure 3.3a reveals a significant problem. Evaluation of the S10C-7GPN mixture over defined portions of the mole fraction regime yield different average β values; beta value above a mole fraction of nonionic of 0.5 is very different than that below a mole fraction of 0.5. To better evaluate the asymmetric CMC pattern, addition ratios for the S10C-7GPN mixture was determined as shown in Figure 3.3b. When β parameters are evaluated independently for low (0-0.4) and high (0.6-1) mole fraction of nonionic 7GPN, both synergism (β of -1.6 for the former range) and antagonism (β of +0.1 for the latter range) was observed. These values are more representative of the actual behavior of this mixture.

This synergism-antagonism pattern as seen in the S10C-7GPN mixture was not clearly observed in any other systems studied, but has been described in the literature previously. For example, Hoffman and Possnecker described it for the tetradecyldimethylamine oxide/ tetraethylammonium perfluoroctanesulfonate binary system [68]. They concluded that the asymmetry of the curve was due to changes in electrostatic and steric interactions produced by variations in micellar composition. Sood et al. [69] observed similar increases in antagonism for stearyldimethyl ammonium chloride/ tetradecyl-benzyl ammonium chloride as the former concentration increased. One possibility is that changes in micelle composition as the nonionic component

increases provide additional surfactant headgroup interaction that hinders micelle formation. For example, it is possible that when the nonionic 7GPN is the major component in the micelle its steric interactions orient the alkanecarboxylate headgroups in a way so as to increase headgroup electrostatic repulsions and cause an antagonistic effect. However, the fact that this effect is not seen in the other mixtures with longer hydrocarbon chain lengths suggests that it might be packing of the hydrophobes within the micelle that causes the loss of synergy at high nonionic contents. Hydrocarbon chain lengths are not the same for the GPN and anionic surfactant, and the relative mismatch between hydrophobe chain lengths will be larger for the shorter molecules which in turn could lead to an antagonistic effect.

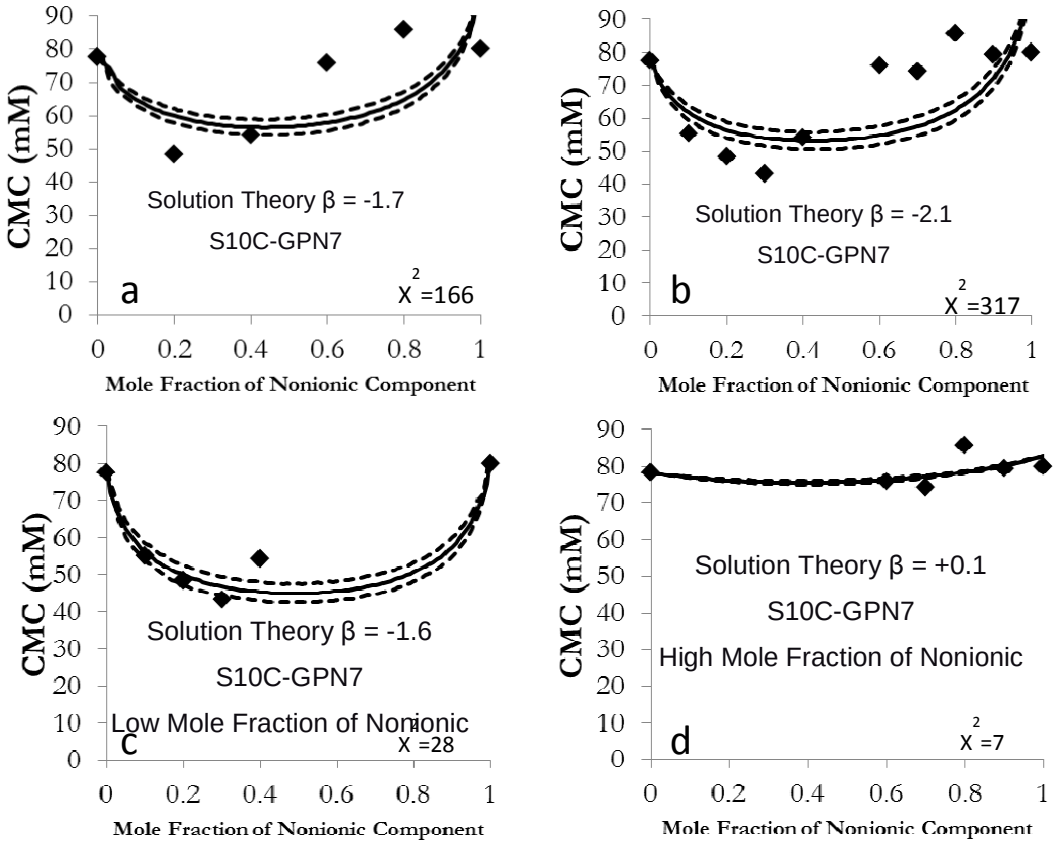

Figure 3.3 Experimental (♦) and predicted (□ □) CMC values as a function of the mole fraction of nonionic component for a) S10C-GPN7 with 6 data points used in the determination using least-squares fitting according to Equations 2 and 3 of the predicted CMC value b) S10C-GPN7 with 10 data points used c) S10C-GPN7 using only 0-0.4 mole fraction of nonionic in the least-squares fit and d) S10C-GPN7 using only 0.6-1 mole fraction of nonionic in the least-squares fit. The solid line is the best fit to the data with dashed lines representing ±10% of the fitted β value.

To further evaluate the effects of nonionic headgroup flexibility on mixed micelle formation, mixtures of sodium n-alkyl carboxylate/glycosides were compared to sodium n-alkyl carboxylate/ N-methylglucamine mixtures as shown in Figure 3.4. Comparing data from Figures 3.2 and 3.3 to that of Figure 3.4, MEGA mixtures showed more negative β parameters than the equivalent GPN mixtures at high and intermediate hydrophobe lengths, consistent with what was found for mixtures with alkyl sulfates. [23] As before, we postulate that this variation in synergism is due to differences in molecular structure which produce variation in flexibility between the two surfactants. Based on a cursory view of Figure 1, the MEGA linear open ring conformation is more able to adopt different conformations. We believe this increased degree of freedom in MEGA headgroup provides more efficient shielding of sodium alkyl carboxylates headgroups, e.g. “wrapping”.

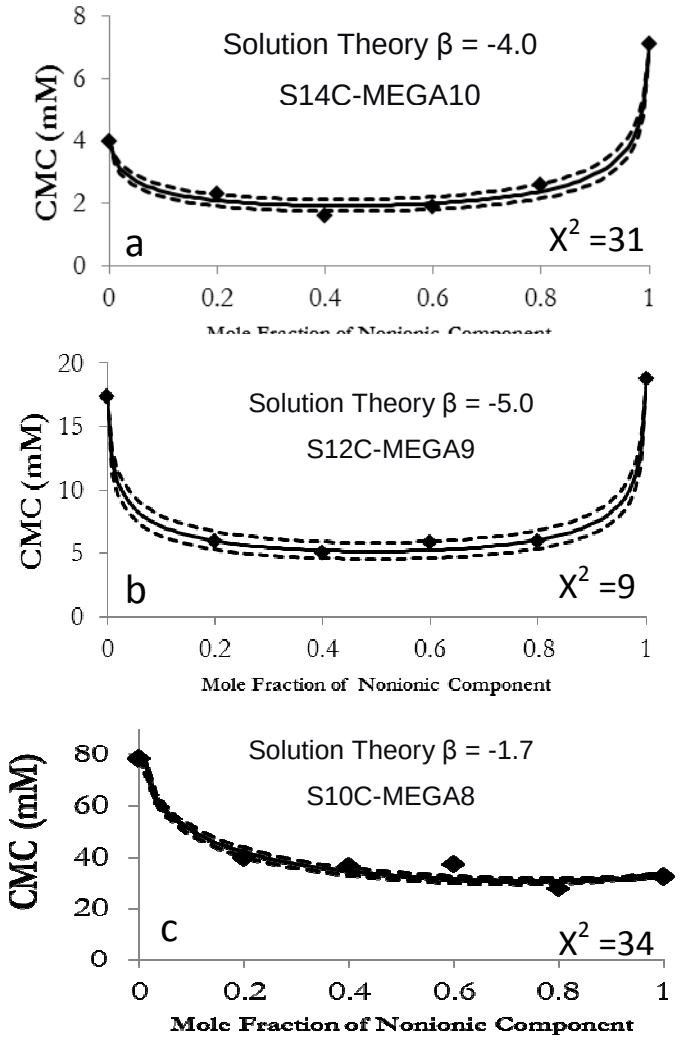

Figure 3.4 Experimental (♦) and predicted (□ □) CMC values for a) S14C-MEGA10 b) S12C-MEGA9 and c) S10C-MEGA8 as a function of the mole fraction of nonionic component. The solid line is the best fit to the data according to Equations 2 and 3, with dashed lines representing ±10% vs. the predicted β value.

3.4Conclusion

The specific objective of this work was to continue our investigation of anionic/nonionic mixtures with respect to their ideality of mixing according to Rubingh's one parameter model for the CMC. The greatest reduction in CMC was found for surfactants with long and intermediate hydrophobe lengths. Low hydrophobe length, carboxylate and glycoside headgroup mixtures produced mixed micelle interactions displaying synergism at low nonionic surfactant mole fractions and slight antagonism at high nonionic mole fractions. The goal of this area of research is to investigate the properties of anionic/nonionic mixtures from renewable resources because of the expected growing importance of highly biocompatible nonionic surfactants from renewable resources and the importance of anionic/nonionic mixtures commercially.

Chapter IV

Effects of pH and Surfactant Precipitation on Surface Tension and CMC Determination of Aqueous Sodium n-Alkyl Carboxylate Solutions

4.1 Introduction

Anionic salts of alkyl carboxylates are used as the primary or secondary surfactant in many commercial formulations. Extensive use of these salts in commercial products is attributed to their desirable physical properties (solubility, wetting, cleaning, etc.), that come in the form of sodium or ammonium salts [10]. The first comprehensive investigations detailing the hydrolysis of anionic sodium alkyl carboxylates in aqueous solution and their formation of different molecular species (i.e. alkanoic acid which are nonionic alkyl carboxylates) at various pH values was presented by Ekwall et al [70-73] and McBain et al [74, 75]. Following Ekwall's and McBain's works, many other studies on soap behavior have been presented as well [5, 42, 76-82].

When dissolved in water, anionic salts of alkyl carboxylates and nonionic alkanoic acid distort the structure of water and therefore increase the free energy of the system. To minimize free energy, at low concentrations surfactant molecules concentrate at the surface, orienting hydrophobic groups away from the solvent. At higher concentrations when the surface nears

surfactant saturation, surface-active molecules (anionic and nonionic surfactant amphiphile) aggregate with their hydrophobic groups directed towards the interior resulting in micelle formation. For any ionic surfactant, the process described above is very sensitive to pH. Micelle formation is an important phenomenon in interfacial interactions such as detergency and solubilization [2]. Micelles in solution affect other interfacial phenomena that do not directly involve micelles such as surface or interfacial tension reduction [2].

As described in chapter III, in addition to numerous authors in the literature [35, 42, 83], issues with the solubility of pure sodium n-alkyl carboxylates in solution near reported critical micelle concentration (CMC) values have been observed. Hence, we decided to once again examine the phase behavior of two important sodium alkyl carboxylates, sodium dodecanoate (S12C) and sodium tetradecanoate (S14C), with the added provision that extensive purification procedures would be performed which have turned out to be important in the determination of the proper CMC of sulfate surfactants [84].

4.2Theoretical Background

Lucassen [85] and Kralchevska et al. [35] previously described the degree of pH sensitivity and different zones of precipitation for sodium n-alkyl carboxylates solutions that result in the formation of neutral-soap, acid-soap and

alkanoic acid crystallites. The carboxylate soap solutions theory developed by Lucassen [85] and generalized by Kralchevska et al. [35] can be used to account for the presence of inorganic electrolytes, base and formation of acid soaps. To predict surfactant precipitation, first consider the following equilibrium of alkanoate dissolution in water [70-72, 74, 75]:

$$Z^- + H_2O \rightleftarrows HZ + OH^- \qquad 4.1$$

$$HZ + Z^- + M^+ \rightleftarrows MZ + MHZ_2 \leftrightarrow \text{precipitate} \qquad 4.2$$

where Z^- is the alkanoate anion, M^+ the metal cation, HZ the alkanoic acid, MZ the neutral soap and MHZ_2 the acid soap. In this study M^+ is Na^+. The equilibriums above are applicable for total surfactant concentrations ($C_T = Z^- + HZ$) both below and above critical micelle concentrations and contain a defined ratio of components Z^-, M^+, HZ, MZ and MHZ_2 at a given C_T.

If no precipitates are present in solution the relationship between C_T and pH of the solution is represented by the following equation [85]:

$$pH \approx 0.5\,[\log(C_T) - \log(K_H K_A)] \qquad 4.3$$

where K_H is equal to the sum of K_W (dissociation constant of water) and K_{CO2} (equilibrium constant of carbon dioxide) and K_A is the dissociation constant of

HZ and can be related to the electroneutrality of the solution through the Debye-Huckel theory.

When considering a simple solution with only alkanoic acid (HZ) precipitation, we have the equation below [85]:

$$pH \approx 0.5\,[\log(C_T) - \log(K_T)] \qquad 4.4$$

were $K_T = K_H + K_{HZ}$ is a constant, and K_{HZ} is the solubility product for HZ. However, as precipitate forms the solution will not only consist of alkanoic acid, but a coexistence of neutral-soap, acid-soap and alkanoic acid crystallites. The exact determination and ratio of surfactant electrolyte constituents will not be determined in this study but are qualitatively evaluated based on visual determination.

4.3Results and Discussion

Table 4.1 shows the CMCs and pC_{20} values found in this study for both pure surfactants as well as various CMC values measured in the literature. The wide range of CMC values for S12C presented in the literature is likely related to the lack of surfactant purity since compounds evaluated in the literature [42, 43, 49, 51, 52, 56] are commonly used as received by the manufacture without additional purification. We initially encountered solubility issues with S12C received at greater than 99% purity for solutions near reported CMC

concentrations at room temperature. However, after recrystallization, purified S12C solutions were soluble at all concentrations (0.01-100 mM) and surface tensions were measured as shown in Figure 4.1. Solubility issues for S14C solution concentrations near reported CMC values were not resolved through additional purification of purchased material. In other words, the CMC could not be measured at room temperature. Wen and Franses [42] reported similar phase behaviors of aqueous S14C at 25˚C, and provide a inferred CMC (4.5 mM) value through ion-selectivity electrodes and conductimetry techniques. However, we believe the "CMC" value reported by Campbell and Lakshminarayanan [43] is not due to micelle formation, but are surface tension breaks caused by the formation of precipitate.

Table 4.1 Chemical name, abbreviation, molecular formula, molecular weight, pC_{20}, CMCs from literature and CMCs measured from this study

Chemical Name	**Abbr.**	**Molecular Formula**	**Molecular Weight (amu)**	**pC_{20}**	**CMC from[2-3] Literature (mM)**	**CMC found[1] in this study (mM)**
Sodium Dodecanoate	S12C	$C_{12}H_{23}NaO_2$	222.3	3.2	21.0^{ST} (20°C),15.0^{ST}(30°C) 28.6^{C}(20°C),26.1^{C}(30°C) 23.0^{ST},25.0^{C},28.1^{C} [43, 49, 51, 52, 56]	19.2
Sodium Tetradecanoate	S14C	$C_{14}H_{27}NaO_2$	250.35	3.7	4.0^{C},$6.9^{ST,C}$, [42, 43]	4.0^{4}

1. All CMC values reported were collected at 25°C. 2. STCMC was obtained by surface tension. 3. ^{C}CMC was obtained by electrical conductivity. 4. Data reported is not a CMC value, but the surfactant concentration at surface tension break caused by the formation of precipitate.

Surface tension reduction efficiency (pC_{20}) is defined as the negative log of the concentration (C_{20}) required to reduce the surface tension of a given solvent by 20 dyne/cm. The pC_{20} is an approximate measure of the minimum surfactant concentration needed to produce saturation adsorption at the interface [86]. The larger the value of $pC_{20,}$ the more efficiently the surfactant is adsorbed at the interface and the more efficiently it reduces surface or interfacial tensions. The efficiency of surfactant in reducing surface tension $-\log C_{20}$, was largest for the longer hydrophobe S14C compared to that of the shorter hydrophobe S12C with reported pC20 values of 3.7 and 3.2 respectively as shown in Figure 4.1. The trend that a higher hydrophobe leads to a larger pC_{20} value has been well established previously and shown to be valid for several homologous series of anionic, cationic, and nonionic surfactants [38, 87-90].

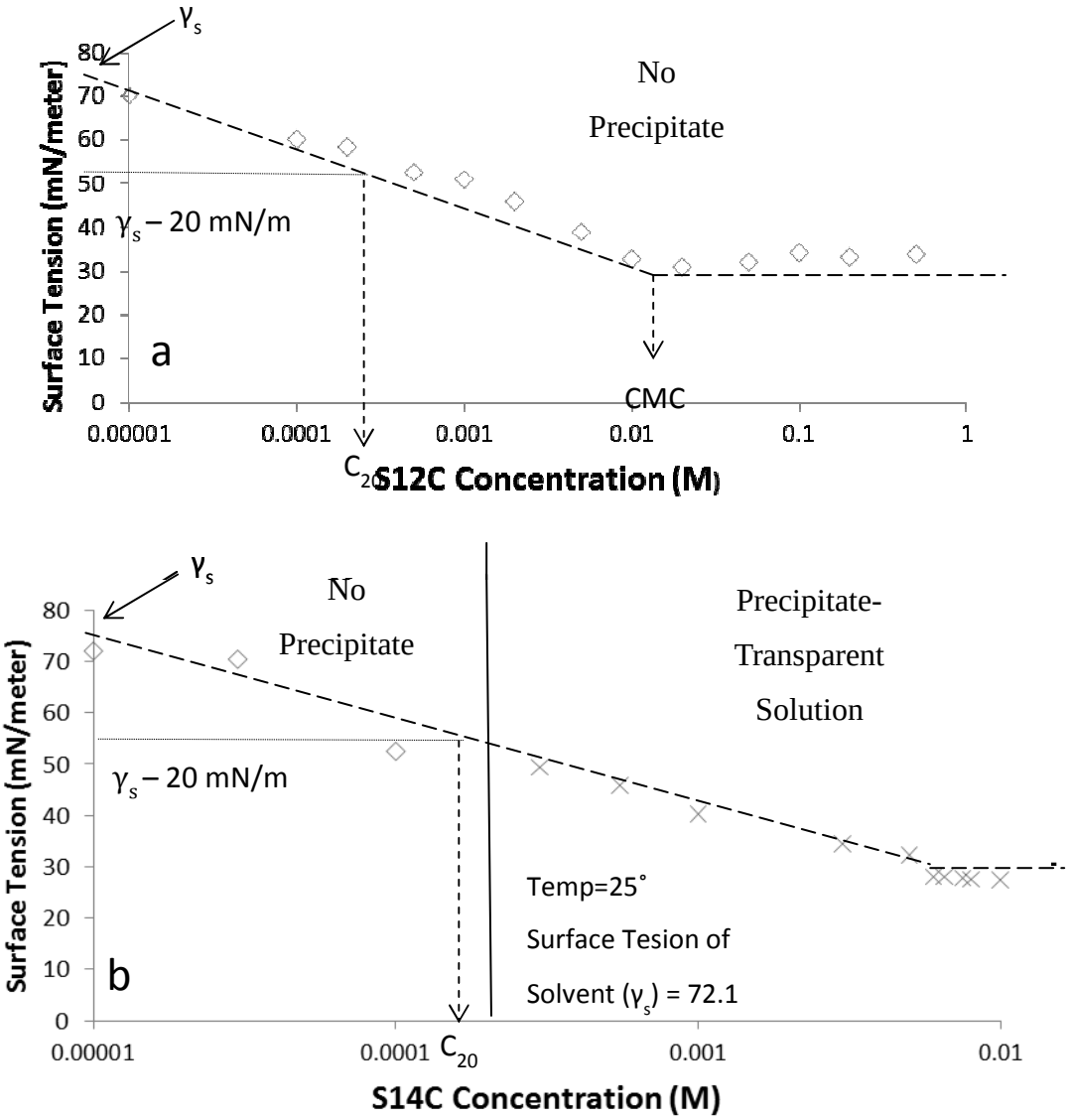

Figure 4.1 Surface tension - log C plot for a) S12C and b) S14C to show how (CMC) and pC_{20} were determined. Dashed lines are fits to data based on a least squares criterion, where (◊) no precipitation-NP, and (X) precipitation-transparent solution-PTS are data points of visual phases. Solid vertical lines determine the boundaries between different precipitate zones.

For S12C and S14C, an increased concentration and dissolution in water is accompanied by an increase in pH due to protonation (hydrolysis) of the oxygen connected to the carbonyl leading to turbidity of the soap solution [35]. As surfactant concentrations were increased there were three visually distinctive precipitation zones. In this study these gross visual appearances were noted as no precipitate (NP), precipitate-transparent solution (PTS) and precipitate-nontransparent solution (PNS) as shown in Figure 4.2.

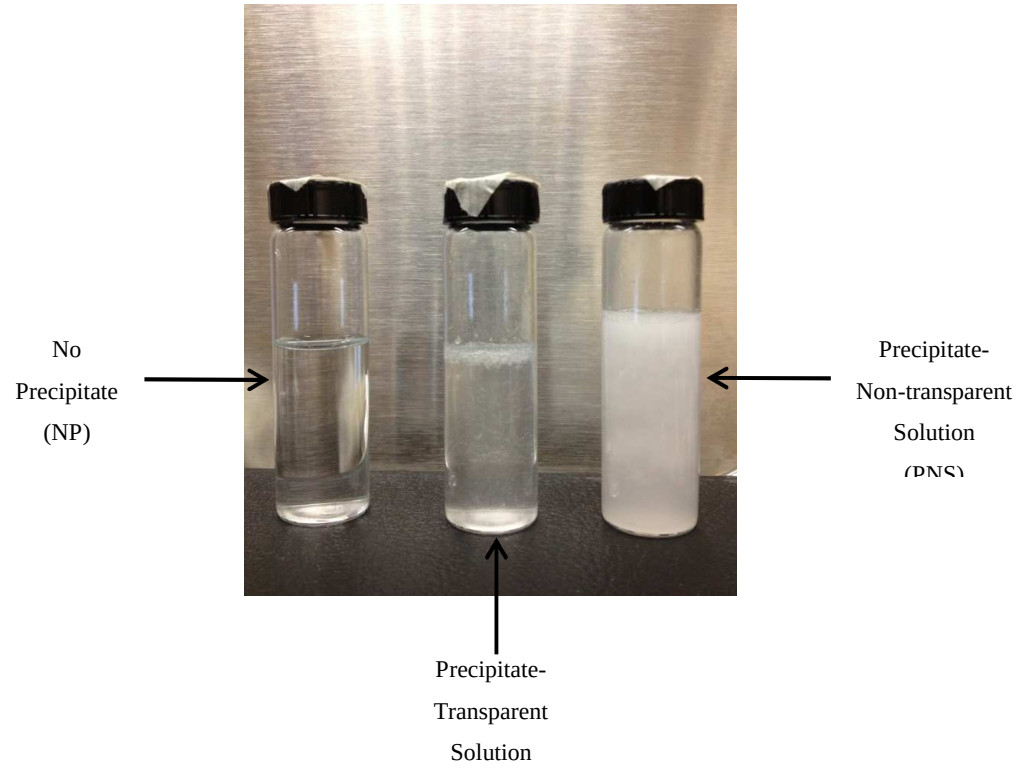

Figure 4.2 Gross visual appearances of pH adjusted surfactant solutions under investigation: no precipitate (NP), precipitate-transparent solution (PTS) and precipitate-nontransparent solution (PNS)

Figure 4.3 a) displays the unadjusted pH and phase behavior of S12C as a function of total surfactant concentration. As determined in the current study and also described in the literature [35, 36, 42, 83, 91], the pH of anionic surfactant solutions gradually increases with an increase in total surfactant concentration. The solution consisted of only one transparent homogeneous phase (NP) absent of precipitate, which allowed for a confident assumption of micelle formation at the determined CMC value presented in Figure 4.1. Kralchevsky et al. [35], describe three precipitation zones at concentrations of 0.01-100mM for S12C. However, the observed precipitation presented in that paper could have been due to the addition of 10 mM sodium chloride.

Figure 4.3 b) displays the pH and phase behavior of S14C as a function of total surfactant concentration. There are two observable precipitation phases (NP and PTS) for the S14C solution, evaluated at a concentrations range of 0.01-10 mM. Kralchevsky et at. [35] observe similar pH trends and provides an extensive description of these precipitation zones based on theoretical analysis. Wen and Franses [42] also report data that shows disperse particles beginning to form around 3 mM and continuing throughout S14C solutions up to 8 mM. It is important to note that both in this study, as well as in the literature, precipitation occurs near solution concentrations previously reported as the experimental CMC for S14C in solution at room temperature.

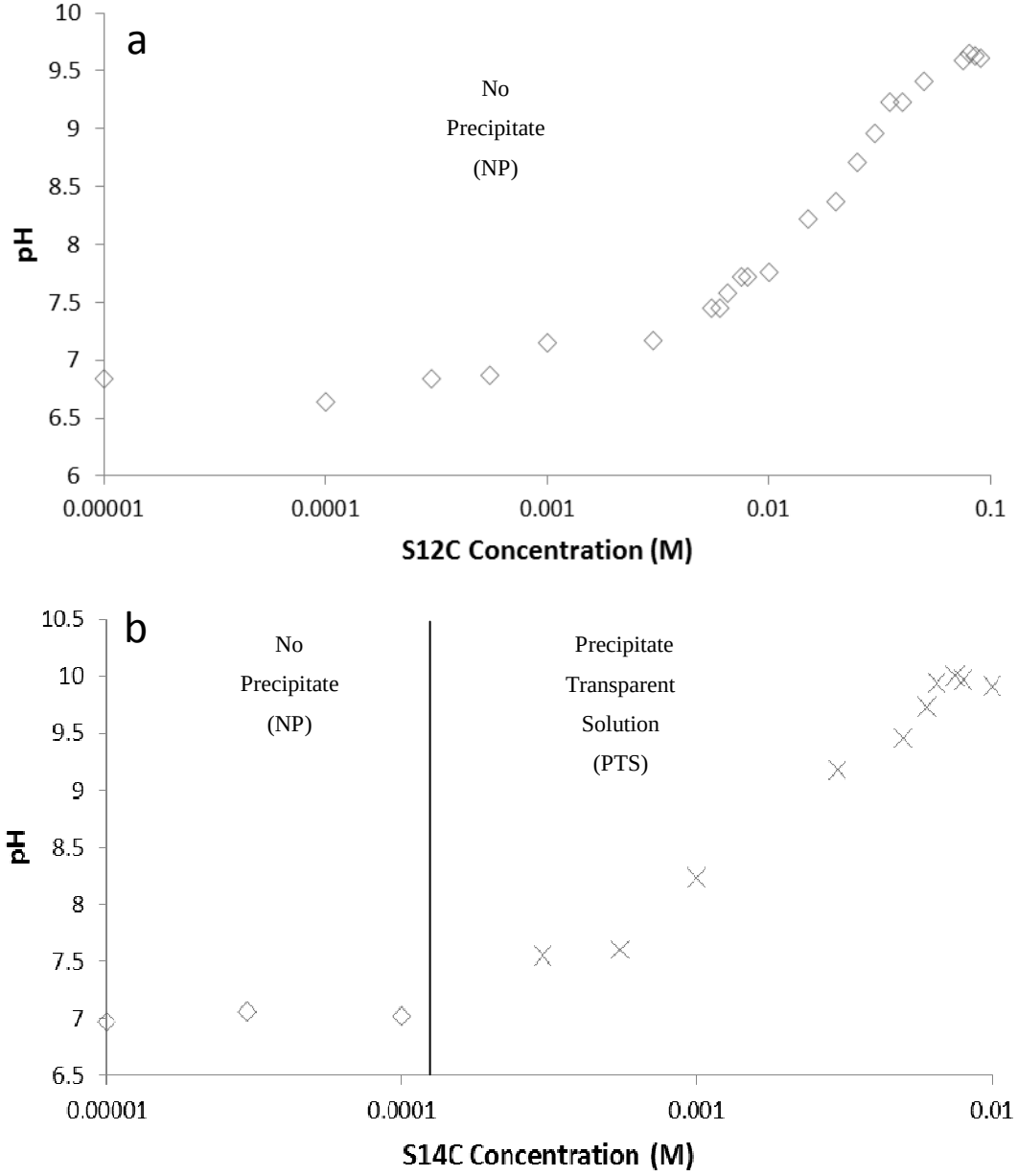

Figure 4.3 pH versus concentration for a) S12C and b) S14C. Solid vertical lines determine the boundaries between zones with different precipitates, where (◊) no precipitation-NP, and (X) precipitation-transparent solution-PTS are data points of visual phases.

We also monitored surface tension variations with pH adjustment for S14C solutions. Figure 4.4 displays the precipitation zones (NP and PNS) and surface tension of S14C versus concentration at six different pH values (pH= 10, 9.5, 9.0, 8.5, 8.0 and 7.5). A depression in surface tension for the NP zone is observed as bulk pH is decreased, a trend also described in the literature for S12C and S14C [36, 92, 93]. This trend can be explained by the increased activity of surfactant at the water-air interface as pK_a values are approached. However, as the optimum surface active 1:1 anionic and nonionic surfactant amphiphile ratio is established, the range of surfactant concentrations in the NP zone decreases and a second PNS zone increases over the evaluated total surfactant concentration. The PNS zone for all solutions had a relatively constant surface tension with an average of 32.6 $\pm$ 0.4 mN/m. This plateau in surface tension is not due to micelle formation but is a product of acid-soap and alkanoic acid crystallites formation. Thus, a standard CMC determination based on micelle formation is not possible for C14S at either natural or adjusted pH for the ranges investigated in this paper.

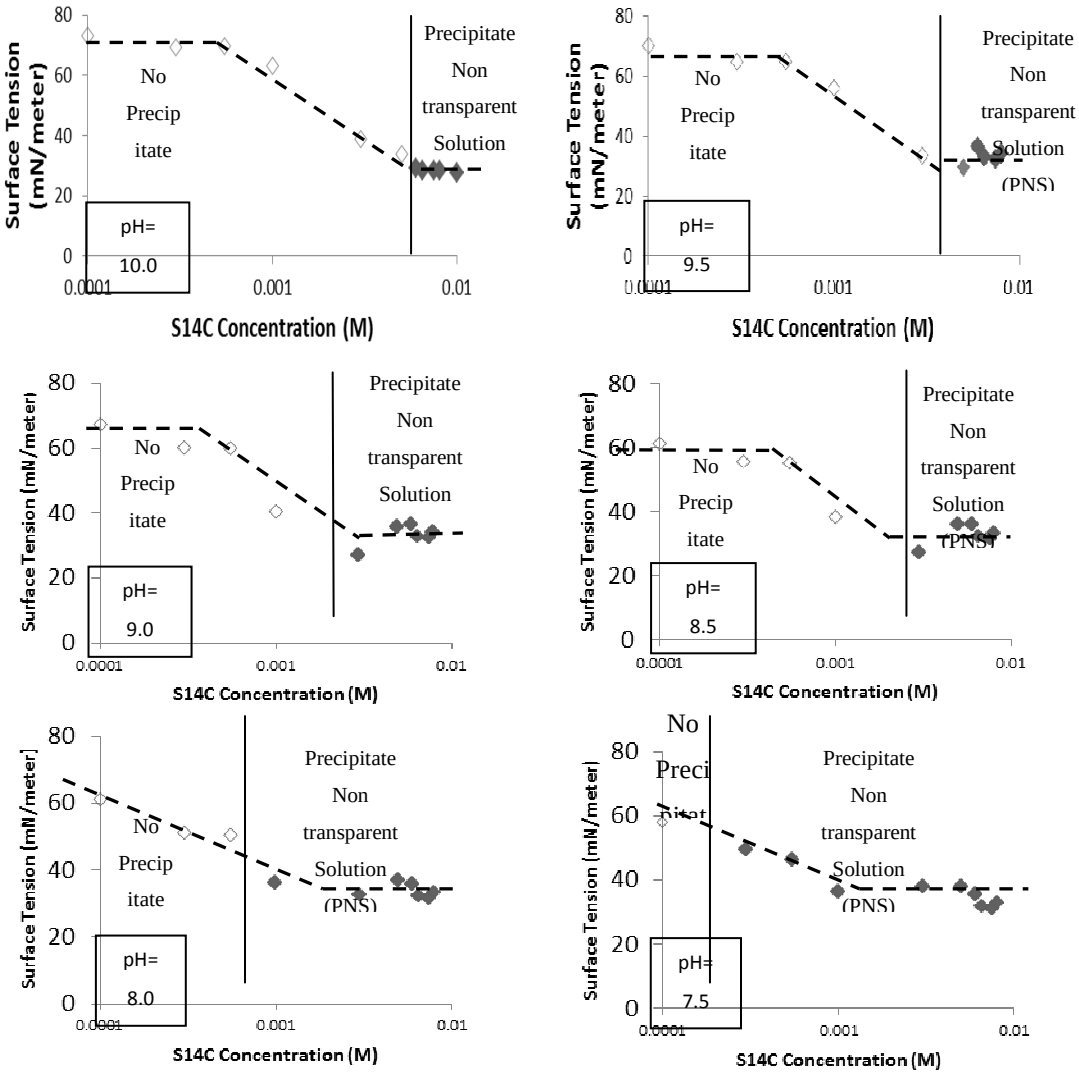

Figure 4.4 Precipitation zones and surface tension of S14C versus concentration, at six different pH values. Solid vertical lines determine the boundaries between the zones with different precipitates, where (◊) no precipitation-NP and (♦) precipitation-nontransparent solution-PNS are data points of visual phases. The dashed line is use to highlight linear relationships found in the data.

Figure 4.5 displays surface tension relationships for defined S14C concentrations. As the trends of surface tension and pH are further examined, interesting relationships between specific pH ranges and surfactant water-air activity is observed. A local minimum in surface tension vs. pH shifts in concentration from 0.55 to 5.0 mM as the concentration increases. Pugh and Stenius [94] also observed a shift in minimum surface tension with increased surfactant concentration. The presence of the minimum has been explained by the hydrolysis and complex formation of oleate dimers, acid soap and by the extremely low solubility of the undissociated acid. Also according to Pugh and Stenius [94] the minimal surface tension for S14C is around pH 9. Our data only agrees with this statement at very specific concentrations; at lower concentrations the minimum is below pH 9 and at high concentration the local minimum shifts above pH= 9 and remains constant between pH 9.5-10.0.

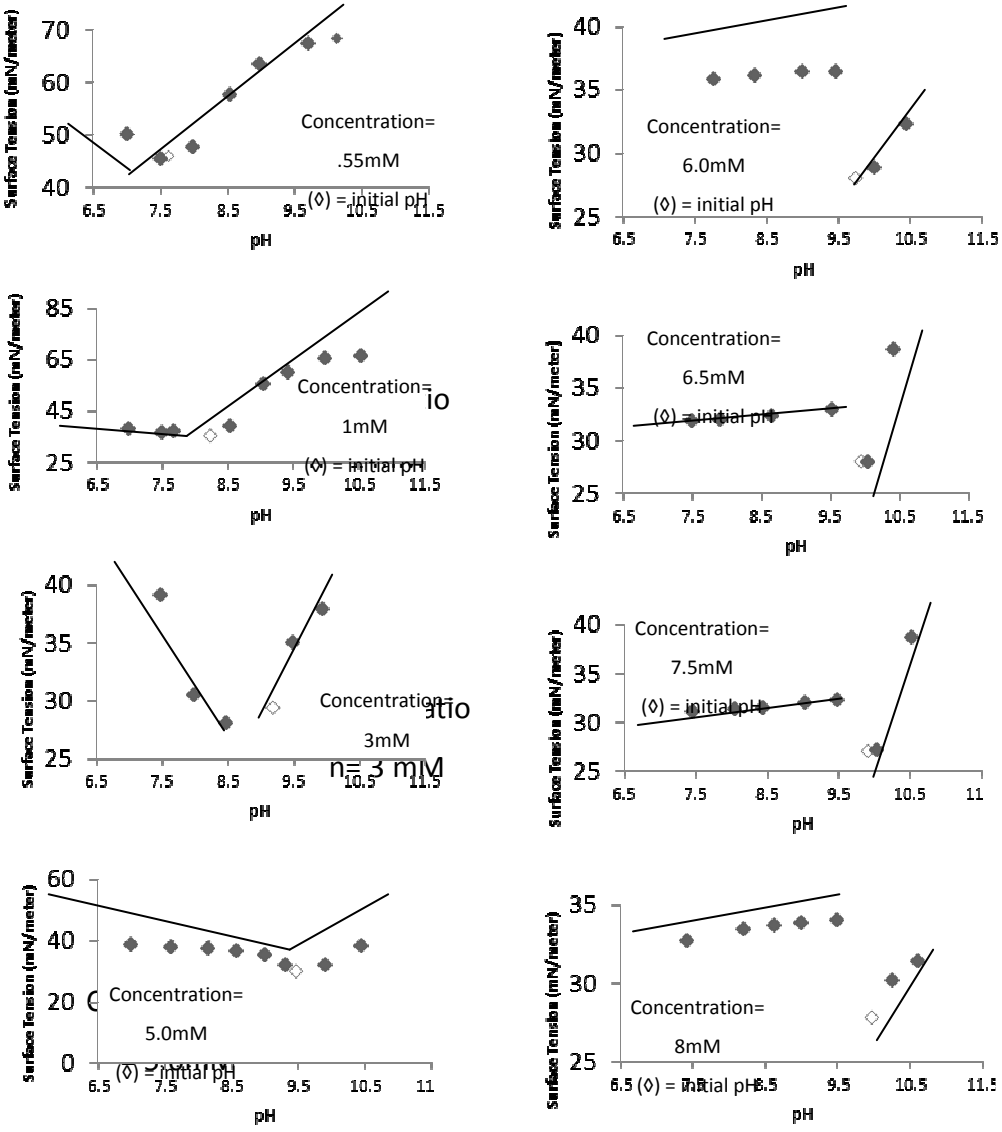

Figure 4.5 Surface tension vs pH at defined S14C concentrations, where (♦) data at increased H_2SO_4 or NaOH concentrations and (◊) data acquired with no additional H_2SO_4 or NaOH. The solid line is used to visually highlight linear relationships found in the data.

4.4Conclusion

As noted in chapter III the S14C and shorter hydrophobe S12C had a degree of pH sensitivity and different zones of precipitation that resulted in the formation of neutral-soap, acid-soap and alkanoic acid crystallites near reported CMC concentrations. Sodium n-alkyl carboxylates are more sensitive to low pH and electrolytes in solution then sulfates, producing comparably higher levels of water-insoluble fatty acids at equivalent pH conditions. Given the solubility issues it was important to explore additional purification techniques and/or define a pH if any that allowed for increased solubility for the given anionic salt systems. Solubility issues encountered with vendor-supplied S12C were resolved through additional purification.

However, solubility for S14C solution concentrations near reported CMC values were not resolved through additional purification or adjustments in bulk pH. It was concluded that observed breaks in surface tension relationships were likely caused by the formation of precipitate not micelle aggregation. As the shift from sulfate to carboxylate headgroup functionality increases in consumer formulations, efforts of effectively and efficiently combining additives for ideal performance at wider pH ranges will continue to be an area of interest.

Chapter V

Determining the Mechanism of Micelle Formation of Binary Surfactant Systems through H^1 NMR Experimentation

5.1 Introduction

In this study Nuclear Magnetic Resonance (NMR) spectrometry experiments were used to probe the underlying intermolecular and intramolecular interactions of binary surfactant systems. Among the experimental techniques available NMR provides a unique advantage of not only providing microscopic information at a molecular level but also provides data about independent behavior of surfactants in the mixed system. NMR spectrometry experiments have increasingly been used to probe the underlying intermolecular and intramolecular interactions of binary surfactant systems [95-99]. Studying and resolving the molecular interactions involved in micelle formation of anionic-nonionic systems will provide insight for optimal formula modifications needed to produce the desired biological and commercial products that utilize the intrinsic properties of surfactants.

5.2 Materials and Methods

In this study surfactants are selected based on structural characteristics (ionic headgroup electron density and nonionic headgroup hydrophobicity).

Sodium dodecyl sulfate (S12S/ alkyl sulfate) is used as the anionic surfactant in mixtures with defined ratios of nonionic, n-Nonyl-β-D-Glucopyranoside (9GPN) constituents. Figure 2.1 shows the molecular structure of surfactants that were used in this study.

All surfactants and their pure CMC values determined through NMR experiments are listed in Table 2. The anionic surfactants possess a hydrophilic headgroup and were mixed with nonionic surfactants made-up of hydrophobic headgroups. S12S was mixed at 9:1 and 1:9 ratio with 9GPN and monitored through NMR proton shifts.

Table 5.1 Chemical name, abbreviation, molecular formula, molecular weight, CMCs from literature and CMCs measured from this study.

Chemical[1] Name	**Abbr.**	**Molecular Formula**	**Molecular Weight**	**CMC from[2-6] Literature (mM)**	**CMC found in this study(mM)[1]**
Sodium Dodecyl Sulfate	S12S	$C_{12}H_{25}SO_4$	288.4	7.9^{ST} ,8.0^{EPR}(20°C),8.2^{ST}, 8.4^{MP} [38-41]	7.0^{7}
n-Nonyl-β-D-Glucopyranoside	9GPN	$C_{15}H_{30}O_6$	306.4	6.5^{NMR}[44]	6.5^{7}

1. Molecular structures of the compounds in the Table are provided in Fig. 1. **2.** All literature CMC values and those found in this study were collected at 25°C. **3.** STCMC was obtained by Surface Tension data. **4.**^{NMR}CMC was obtained by chemical shift coefficients of methyl group protons. **5.** ^{MP}CMC was obtained by membrane potential studies. **6.** ^{EPR}CMC was obtained by evaluation of electron paramagnetic resonance **7.** CMC measured in this study by NMR.

5.3 Theory

As first described and measured by Rabi [100] the spin state of selected nuclei within molecules are exploited to evaluate their molecular interaction in solution [101]. Arranging randomly in solution, surfactant proton nuclei spin and orient in a +1/2(α) or -1/2(β) spin state when exposed to an external magnetic field. The two spin states have different energies that diverge with the increase of external magnetic field strength. Just over half of the nuclei exist in the lower +1/2(α) energy state. Since more spins are in the +1/2(α) than -1/2(β) orientation a net magnetization is produced. When energy in the form of a pulse (oscillating magnetic field) is applied to the system two events happen, first the energy difference is removed and second the spins are aligned (in phase). Under these conditions the net magnetization is perpendicular to the applied field. Over time the energy difference and spin alignment return to their initial distribution and their spins come out of alignment processes termed reequilibration (longitudinal relaxation) and dephasing (transverse relaxation). The coil that applies the pulse is also used to detect the energy released by the protons as they return to the equilibrium established by the external magnetic field. The motions of the protons released energy as they return to equilibrium constitute a radio-frequency signal. The decaying signal contains the sum of the frequency from all the target nuclei. The magnitude of the energy changes involved in NMR spectroscopy is very small. To increase sensitivity multiple spectra are taken and

data is added, reducing noise. The one dimensional NMR experiment used the following sample pulse sequence:

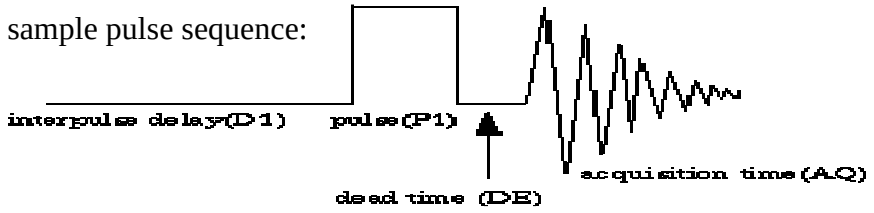

Figure 5.1 1H NMR experiments parameter values: delay (D1-0.010 sec), pulse (P1-0.005 sec, 75.4°) and acquisition time (AQ-1.364 sec). Each mixture had a total of 32 sequential pulse sequences conducted with a total experiment time of forty three seconds.

The electrons surrounding the protons also experience induced magnetic fields. The observed chemical shifts between protons located in different electronic environments within the molecule are a result of these electron induced magnetic fields. For example, protons alpha and beta to the oxygen of the sulfate in S12S are in less dense magnetic fields (deshielded) relative to the other alkyl protons and producing signature signal farther downfield as seen in Figure 5.2. Surfactant concentrations also produce changes in surfactant proton environment, resulting in detectable shifts of proton signals which are used to determine surfactant CMCs.

In aqueous solution the change in chemical shift is directly related to the motional behavior of the surfactant molecule as it exists as monomer or in micelle. When the surfactant molecule aggregates to form micelles, their

motions slow down and the correlation time becomes longer, and the observed chemical shifts become faster. Due to the fast exchange between the monomer and micelle the observed chemical shift is a weighted average between monomer and micelle expressed as followed [95]:

$$\delta_{obsd} = \left(\frac{C_{mon}}{C_T}\right)\delta_{mon} + \left(\frac{C_{mic}}{C_T}\right)\delta_{mic} \qquad 5.1$$

were δ_{obsd}, δ_{mon} and δ_{mic} are the observed chemical shift, chemical shifts of the micelle and the monomer chemical shift, respectively. C_{mon} and C_{mic} are the concentrations of the monomer and the micelle with C_T representing the total concentration (C_{mon}+ C_{mic}). The independent CMC for each surfactant in solution can be obtained if it is assumed that at concentrations below the CMC the chemical shift equals monomer concentration (Eq. 5.2) and above the CMC the monomer concentration is constant and equals the CMC (Eq. 5.3).

$$\delta_{obsd} = \delta_{mon} \ (C_T < CMC) \qquad 5.2$$

$$\delta_{obsd} = \frac{(\delta_{mon} - \delta_{mic})CMC}{C_T} + \delta_{mic} \ (C_T > CMC) \qquad 5.3$$

Three lines are produced by plotting the observed monomer and micelle chemical shift versus the reciprocal surfactant total concentration as displayed in

Figure 5.2. The slopes of lines one and three are 0 and (δ_{mon}- δ_{mic})CMC for line two. The intersection of line one and two is the CMC. The observed change in slope and intersection of chemical shifts represents the transition in surfactant environment from aqueous to micelle aggregates and are used to construct phase diagrams.

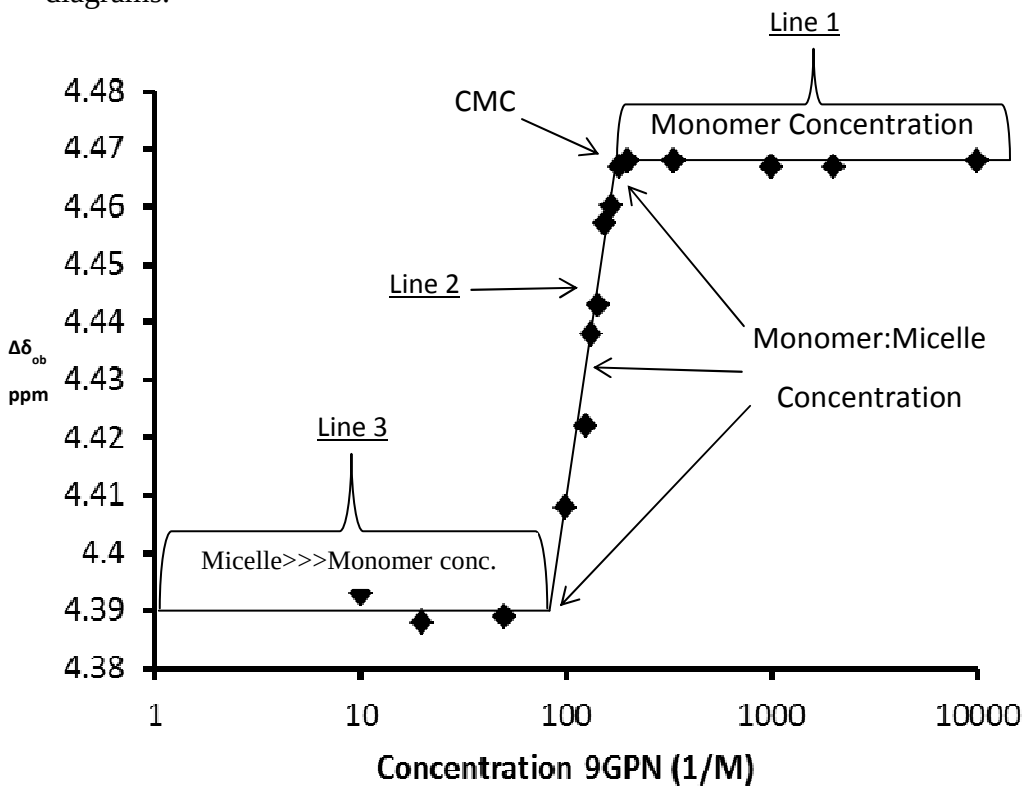

Figure. 5.2 Variation of $(\delta)_{obsd}$ versus the reciprocal concentration of pure 9GPN, were the diamonds (♦) are experimental data points and the solid lines (—) are used to guide the eye along liner relationships.

5.4Data

A VNMRS 500 MHz-NMR Spectrometer figure 5.3 was used to collect NMR data. Chemical shifts are expressed in ppm using residual solvent protons as an internal standard (0.00 for DSS). Figure 5.3 displays the absolute assignment of proton shifts for pure S12S, 9:1 S12S-9GPN, 1:9 S12S-9GPN and pure 9GPN at a 6mM concentration. The CMC of pure and binary surfactant systems were determined by analyzing changes in observed chemical shift $(\delta)_{obsd}$ of resonance peaks. The CMC was obtained by plotting the change in chemical shift versus the reciprocal concentration and observing defined breaks as shown in Figure 5.4.

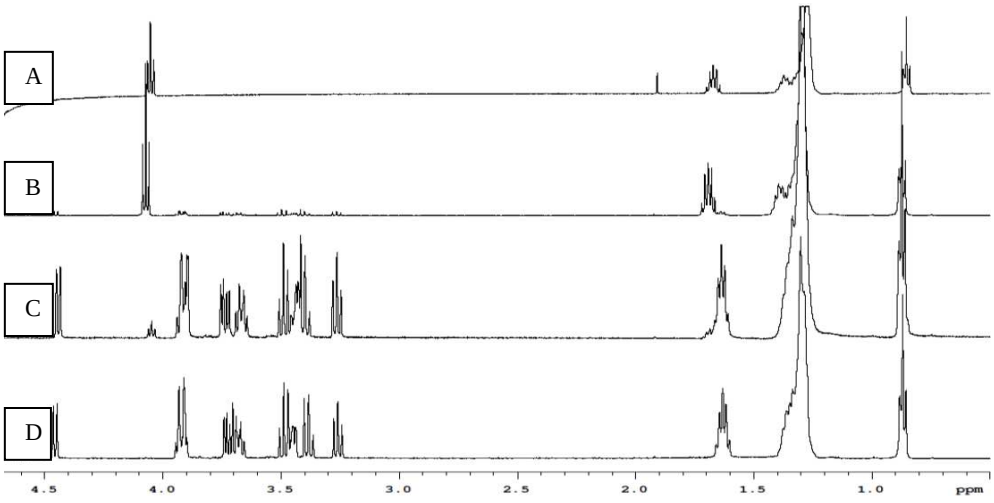

Figure 5.3 ^{1}H NMR spectra and assignment of 6mM solutions of (A) pure S12S, (B) 9:1 S12S-9GPN, (C) 1:9 S12S-9GPN, and (D) pure 9GPN in D2O at 25°C.

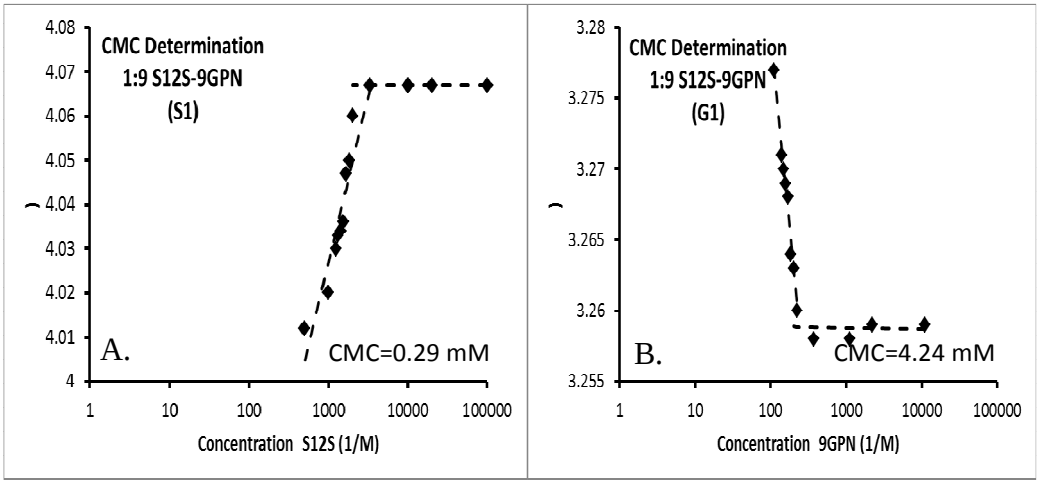

Figure 5.4 Variation of $(\delta)_{obsd}$ versus the reciprocal concentration for (A) 9:1 S12S-9GPN and (B) 1:9 S12S-9GPN mixtures, were the diamonds (♦) are experimental data points and the solid lines (—) are used to guide the eye along liner relationships.

Analyses of proton chemical shifts were conducted to determine experimental aggregation concentrations of each surfactant in the mixture provided in Table 1. The experimental CMC data and predetermined mixture ratios were then used to calculated the concentrations of the second substituent in the define surfactant system. The sum of the experimental CMC and concentration of the second substituent were calculated to determine the total surfactant concentration at aggregation. From CMC data collected through 1D NMR experiments phase diagrams were constructed as displayed in Figure 5.5.

Table 5.2 Surfactant micelle formation and CMC data for 9:1 and 1:9 S12S-GPN9 determined through Proton NMR experiments.

9:1 S12S-9GPN	Proton (S1)	Proton (S2)	CMC mM	Total Concentration mM
S12S	4.98 ± 0.11mM	4.93 ± 0.13mM	4.96[1] (0.55)*	5.51
	Proton (G1)	**Proton (G1')**		
GPN9	0.53 ± 0.045mM	0.56 ± 0.047mM	0.54[2] (4.86)*	5.40
1:9 S12S-GPN9	**Proton (S1)**	**Proton (S2)**	**CMC mM**	**Total Concentration mM**
S12S	0.29 ± 0.036mM	--	0.29[2] (2.61)*	2.90
	Proton (G1)	**Proton (G1')**		
GPN9	4.24 ± 0.085mM	4.23 ± 0.080mM	4.24[1] (0.47)*	4.71

[1]The mixed CMC value determined by analysis of observed proton chemical shifts $(\delta)_{obsd.}$ [2]The pure ionic micelle formation value determined by analysis of observed proton chemical shifts $(\delta)_{obsd.}$ *The calculated molar concentration of the second substituent in the defined surfactant ratios. The standard deviations (STDEV) were calculated by averaging values for fits to 3:3, 4:4, 5:5 and 6:6 high[1/M]-low[1/M] data based on a least squares criterion.

As observed in the Cui [95] etc., in a cationic-nonionic system a pure micelle aggregate is formed at a concentration below the mixed CMC. In addition to observing non-stepwise mixed micelle formation, the data suggest a novel third monomer-micelle phase as shown in Figure 5.5. The intrinsic properties (synergy) of the mixed surfactants drive step II which corresponds to the initiation of region III. However, this mechanism does not explain the pure micelle formation in region II. To explain this concentration regime, we first

look at region I in which both surfactants are monomers and completely dispersed in solution. When dissolved in water surfactants hydrophobic groups distort the structure of water and therefore increase the free energy of the system. To minimize free energy, at low concentrations surfactant molecules concentrate at the surface, orienting hydrophobic groups away from the solvent. At higher concentrations when the surface nears surfactant saturation, surface-active molecules aggregate with their hydrophobic groups directed towards the interior resulting in micelle formation.

However, because the nonionic surfactant headgroup is large and hydrophobic relative to the ionic headgroup it is possible that it begins to forms bilayers at step I. With limited access to nonionic bilayer insertion, anionic surfactants aggregate into pure micelles to produce a decrease in free energy at step I. As concentrations increase the nonionic bilayer saturates and the repulsive forces of the anionic micelle increases. To reduce repulsive forces, the nonionic surfactants begin to fuse into the pure ionic aggregate forming mixed micelles at step II.

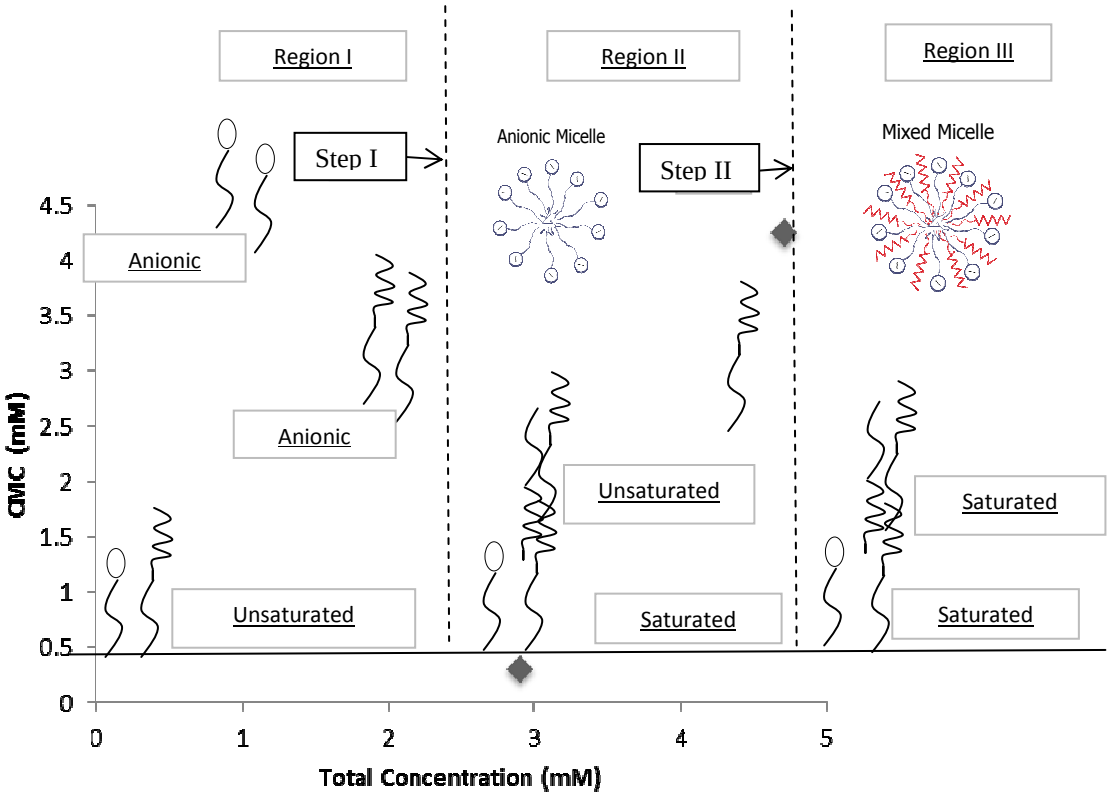

Figure 5.5 Phase Diagram of micelle formation for a 1:9 S12S-GPN9 mixture.

Based on the proposed mechanism when the mixture is at a 9:1 S12S-9GPN the system experiences a relatively small or nonexistent bilayer at the water/surface interface. Thus, upon surface saturation in a 9:1 S12S-9GPN mixture the system forms mixed micelles in a non-stepwise manner excluding step I and region II. However, in the 1:9 S12S-GPN9 mixture when the nonionic surfactant is the major component a relatively large nonionic bilayer is produced forming an observable region II. The preliminary results provide invaluable insight into the possible molecular interactions experienced near concentrations at which mixed micelle are formed.

5.5Conclusion

Nuclear magnetic resonance (NMR) experiments were used to evaluate binary anionic-nonionic surfactant systems at various concentrations and mixture ratios. Both stepwise and non-stepwise micelle formation was observed. The realization of a stepwise mechanism questions the assumption of non-stepwise mixed micelle formation ignored or assumed by all models and theories currently used in the literature, and suggest a novel binary surfactant interaction. As shown in chapter 5.5 these compositional relationships can be used to produce phase diagrams to evaluate the molecular interactions of electronic and structurally selected anionic-nonionic aqueous mixtures. The current work will ultimately provide better theoretical tools needed for the optimal selection and evaluation of amphiphilic molecules used in scientific, commercial and industrial research and development.

Chapter VI

Conclusion and Recommendations

6.1 Conclusion

The results from the present studies demonstrate that complex interactions of mixed anionic-nonionic system are dependent on, but not necessarily limited to, nonionic hydrophile size/flexibility and anionic group. It was also shown that purification of vendor supplied surfactant is important in the accurate CMC determination of S12C. However, solubility for S14C solution concentrations near reported CMC values were not resolved through additional purification of purchased material. CMC values reported in the literature for C14S should be reconsidered, as breaks in surface tension relationships are likely caused by the formation of precipitate not micelle aggregation. Also, through NMR spectroscopy experiments a stepwise mechanism for micelle formation in mixed systems was observed. The observed stepwise mechanism suggest a novel binary surfactant interaction.

6.2 Recommendations

Further development for the mechanism of micelle formation present in Chapter 5 can be achieved through ^{1}H NMR experiments of additional binary system selected based on variations of nonionic headgroup size and flexibility. Improved understanding of the underlying inter- and intra- molecular forces will

reduce time and materials needed for experimental evaluation of various amphiphilic molecules. With the use of methodology presented in Chapter 5 binary systems of sodium dodecyl sulfate (S12S/ alkyl sulfate) mixed with Decanoyl-N-Methylglucamide (MEGA10) and n-Nonyl-β-D-Maltopyranoside (2GPN) should be evaluated through ^{1}H NMR experiments.

As discussed in Chapter 5 when mixed at a 1:9 anionic/nonionic ratios the electron density of the ionic surfactant and the molecular structure of nonionic surfactant are predicted to cause critical micelle aggregation at two different total surfactant concentrations. The first total surfactant concentration will consist of pure ionic micelles and dispersed nonionic monomer. While the second total surfactant concentration will contain mixed ionic-nonionic micelles and occur at a higher total surfactant concentration than the first surfactant aggregation concentration. When MEGA10 (most molecularly flexible nonionic surfactant) is the major component mixed with S12S, it is predicted to produce the largest difference between total surfactant concentration containing pure ionic micelles relative to the mixed micelle total concentration. Comparatively, a 1:9 S12S-2GPN9 mixture should display the smallest difference in total surfactant concentrations containing pure ionic micelle aggregates compared to total mixed micelle concentration.

The MEG10 is the most flexible nonionic headgroup containing polar hydroxyl groups. However, it is in the smaller size grouping of the three

suggested. The 9GPN has relatively the same amount of hydroxyl substitution however; the degree of headgroup flexibility is limited due to its more ridged six-member ring major confirmation. The largest of the three is the 2GPN9, consisting of the greatest hydroxyl substitution. Base on proposed mechanism for Figure 5.3 it is predicted that the magnitude of the percent reduction of total surfactant concentrations containing pure ionic micelles will display the following trend for 1:9 anionic/nonionic mixtures: S12S-MEGA10 > S12S-9GPN > S12S-2GPN9. Experiments should be performed to prove this assertion.

6.3 References

1. Rosen M (2004) Surfactant and Interfacial Phenomena.

2. Zhou Q and Rosen MJ (2003) Molecular Interactions of Surfactants in Mixed Monolayers at the Air/Aqueous Solution Interface and in Mixed Micelles in Aqueous Media: The Regular Solution Approach. Langmuir 19: 4555-4562

3. Porter M (1997) Handbook of Surfactants.

4. R B (1997) Kirk-Othmers Encyclopedia of Chemical Technologies.

5. Lynch ML, Wireko F, Tarek M and Klein M (2001) Intermolecular Interactions and the Structure of Fatty Acid-Soap Crystals. J Phys Chem B 105: 552-561

6. M S (2006) Handbook of Detergents.

7. E. S (2002) Laundry Detergent.

8. Hoydonckx HE, De Vos DE, Chavan SA and Jacobs PA (2004) Esterification and Transesterification of Renewable Chemicals. Top Catal 27: 83-96

9. Freitas L, Paula AV, dos Santos JC, Zanin GM and de Castro HF (2010) Enzymatic Synthesis of Monoglycerides by Esterification Reaction Using Penicillium Camembertii Lipase Immobilized on Epoxy Sio2-Pva Composite. J Mol Catal B-Enzym 65: 87-90

10. Zoller U (2009) Handbook of Detergents. Part E: Applications 141-145: 469

11. Fendler (1975) Catalysis in Micellar and Macromolecular Systems.

12. Mukerjee P. MK (1971) Critical Micelle Concentrations of Aqueous Surfactant Systems.

13. T. W (1968) Adsorption from Aqueous Solution.

14. Osterhof HJ and Bartell FE (1930) Three Fundamental Types of Wetting Adhesion Tension as the Measure of Degree of Wetting. J Phys Chem 34: 1399-1411

15. Matsumoto S, Kita Y and Yonezawa D (1976) Attempt at Preparing Water-in-Oil-in-Water Multiple-Phase Emulsions. J Colloid Interface Sci 57: 353-361

16. Kitchener JA and Cooper CF (1959) Current Concepts in the Theory of Foaming. Quarterly Reviews 13: 71-97

17. Holmberg K (2001) Natural Surfactants. Curr Opin Colloid Interface Sci 6: 148-159

18. von Rybinski W and Hill K (1998) Alkyl Polyglycosides - Properties and Applications of a New Class of Surfactants. Angew Chem-Int Edit 37: 1328-1345

19. Rosen MJ and Hua XY (1982) Synergism in Binary-Mixtures of Surfactants .2. Some Experimental-Data. J Am Oil Chem Soc 59: 582-585

20. Rosen MJ (1989) Selection of Surfactant Pairs for Optimization of Interfacial Properties. J Am Oil Chem Soc 66: 1840-1843

21. Rosen MJ (1986) Molecular Interaction and Synergism in Binary-Mixtures of Surfactants. Acs Sym Ser 311: 144-162

22. Scamehorn JF (1986) An Overview of Phenomena Involving Surfactant Mixtures. Acs Sym Ser 311: 1-27

23. Werts KM and Grady BP (2011) Mixtures of Nonionic Surfactants Made from Renewable Resources with Alkyl Sulfates: Comparison of Headgroups. J Surfactant Deterg 14: 77-84

24. Liebert MA (1983) Assessment of Sodium Lauryl Sulfate. Journal of The American College of Toxicology 2: 127

25. Herlofson BB and Barkvoll P (1994) Sodium Lauryl Sulfate and Recurrent Aphthous Ulcers - a Preliminary-Study. Acta Odontol Scand 52: 257-259

26. Herlofson BB and Barkvoll P (1996) The Effect of Two Toothpaste Detergents on the Frequency of Recurrent Aphthous Ulcers. Acta Odontol Scand 54: 150-153

27. Shinoda K (1954) The Critical Micelle Concentration of Soap Mixtures (2-Component Mixture). J Phys Chem 58: 541-544

28. Lange H and Beck KH (1973) Micelle Formation in Mixed Solutions of Homologous and Non-Homologous Surface-Active Agents. Kolloid-Zeitschrift and Zeitschrift Fur Polymere 251: 424-431

29. Clint JH (1975) Micellization of Mixed Nonionic Surface-Active Agents. Journal of the Chemical Society-Faraday Transactions I 71: 1327-1334

30. Rubingh (1979) Solution Chemistry of Surfactants. 1:

31. Rosen MJ (1984) Structure/Performance Relationships in Surfactants. ACS Symposium Series 253: 141-151

32. Rathman JF and Scamehorn JF (1988) Determination of the Heat of Micelle Formation in Binary Surfactant Mixtures by Isoperibol Calorimetry. Langmuir 4: 474-481

33. Maeda H (1995) A Simple Thermodynamic Analysis of the Stability of Ionic Nonionic Mixed Micelles. J Colloid Interface Sci 172: 98-105

34. Puvvada S and Blankschtein D (1992) Thermodynamic Description of Micellization, Phase-Behavior, and Phase-Separation of Aqueous-Solutions of Surfactant Mixtures. J Phys Chem 96: 5567-5579

35. Kralchevsky PA, Danov KD, Pishmanova CI, Kralchevska SD, Christov NC, Ananthapadmanabhan KP and Lips A (2007) Effect of the Precipitation of Neutral-Soap, Acid-Soap, and Alkanoic Acid Crystallites on the Bulk Ph and Surface Tension of Soap Solutions. Langmuir 23: 3538-3553

36. Theander K and Pugh RJ (2001) The Influence of Ph and Temperature on the Equilibrium and Dynamic Surface Tension of Aqueous Solutions of Sodium Oleate. J Colloid Interface Sci 239: 209-216

37. Decastro FHB and Borrego AG (1995) Modification of Surface-Tension in Aqueous-Solutions of Sodium Oleate According to Temperature and Ph in the Flotation Bath. J Colloid Interface Sci 173: 8-15

38. Dahanayake M, Cohen AW and Rosen MJ (1986) Relationship of Structure to Properties of Surfactants .13. Surface and Thermodynamic Properties of Some Oxyethylenated Sulfates and Sulfonates. Journal of Physical Chemistry 90: 2413-2418

39. Wasserman AM, Motyakin MV, Yasina LL, Zakharova YA, Matveenko VN, Shulevich YV and Rogovina LZ (2010) Epr Spin Probe Study of New Micellar Systems. Appl Magn Reson 38: 117-135

40. Elworthy PH and Mysels KJ (1966) Surface Tension of Sodium Dodecylsulfate Solutions and Phase Separation Model of Micelle Formation. J Colloid Interface Sci 21: 331-&

41. Ingram T and Jones MN (1969) Membrane Potential Studies on Surfactant Solutions. Transactions of the Faraday Society 65: 297-&

42. Wen XY and Franses EI (2000) Effect of Protonation on the Solution and Phase Behavior of Aqueous Sodium Myristate. J Colloid Interface Sci 231: 42-51

43. Campbell AN and Lakshmin.Gr (1965) Conductances and Surface Tensions of Aqueous Solutions of Sodium Decanoate Sodium Laurate and Sodium Myristate at 25 Degrees and 35 Degrees. Can J Chem 43: 1729-&

44. De Grip WJ and Bovee-Geurts PHM (1979) Synthesis and Properties of Alkyl Glucosides with Mild Detergent Action Improved Synthesis and Purification of Beta-1 Octyl Glucose Beta-1 Nonyl Glucose and Beta-1 Decyl Glucose Synthesis of Beta-1 Undecyl Glucose and Beta-1 Dodecyl Maltose. Chem Phys Lipids 23: 321-336

45. Anatrace (2009-2010) Catalogue (Affymetrix) 2009.

46. Hierrezuelo JM, Aguiar J and Ruiz CC (2004) Stability, Interaction, Size, and Microenvironmental Properties of Mixed Micelles of Decanoyl-N-Methylglucamide and Sodium Dodecyl Sulfate. Langmuir 20: 10419-10426

47. Walter A, Suchy SE and Vinson PK (1990) Solubility Properties of the Alkylmethylglucamide Surfactants. Bioch Et Biophy Acta 1029: 67-74

48. Hanatani M, Nishifuji K, Futai M and Tsuchiya T (1984) Solubilization and Reconstitution of Membrane-Proteins of Escherichia-Coli Using Alkanoyl-N-Methylglucamides. J Biochem 95: 1349-1353

49. Alvarez-Silva E, Garcia-Abuin A, Gomez-Diaz D, Navaza JM and Vidal-Tato I (2010) Density, Speed of Sound, Surface Tension, and Electrical Conductivity of Sodium Dodecanoate Aqueous Solutions from T = (293.15 to 323.15) K. J Chem Eng Data 55: 4058-4061

50. Blanco E, Gonzalez-Perez A, Ruso JM, Pedrido R, Prieto G and Sarmiento F (2005) A Comparative Study of the Physicochemical Properties of Perfluorinated and Hydrogenated Amphiphiles. J Colloid Interface Sci 288: 247-260

51. Rodriguez-Pulido A, Casado A, Munoz-Ubeda M, Junquera E and Aicart E (2010) Experimental and Theoretical Approach to the Sodium Decanoate-Dodecanoate Mixed Surfactant System in Aqueous Solution. Langmuir 26: 9378-9385

52. DeLisi R, Inglese A, Milioto S and Pellerito A (1996) Thermodynamic Studies of Sodium Dodecyl Sulfate Sodium Dodecanoate Mixtures in Water. J Colloid Interface Sci 180: 174-187

53. Lorber B, Bishop JB and Delucas LJ (1990) Purification of Octyl Beta-D-Glucopyranoside and Reestimation of Its Micellar Size. Biochim Biophysica Acta 1023: 254-265

54. Chattopadhyay A and London E (1984) Fluorimetric Determination of Critical Micelle Concentration Avoiding Interference from Detergent Charge. Anal Biochem 139: 408-412

55. Delisi R, Perron G and Desnoyers JE (1980) Volumetric and Thermochemical Properties of Ionic Surfactants - Sodium Decanoate and Octylamine Hydrobromide in Water. Can J Chem 58: 959-969

56. Blanco E, Gonzalez-Perez A, Ruso JM, Pedrido R, Prieto G and Sarmiento F (2005) A Comparative Study of the Physicochemical Properties of Perfluorinated and Hydrogenated Amphiphiles. Journal of Colloid and Interface Science 288: 247-260

57. Andrade-Dias C, Lima S and Teixeira-Dias JJ (2007) From Simple Amphiphilic to Surfactant Behavior: Analysis of H-1 Nmr Chemical Shift Variations. J Colloid Interface Sci 316: 31-36

58. Ko JS, Oh SW, Kim KW, Nakashima N, Nagadome S and Sugihara G (2005) Blending Effects on Adsorption and Micellization of Different Membrane Protein Solubilizers: A Thermodynamic Study on Three Mixed Systems of Chaps with Mega-8,-9 and-10 in Ph 7.2 Phosphate Buffer Solution. Colloid Surf B-Biointerfaces 45: 90-103

59. Traube I (1903) The Physical Properties of Elements, from the Standpoints of Van Der Waal's Equation of States. Z Anorg Chem 34: 413-426

60. Kling W and Lange H (1957) Grenzflachenspannung Wassriger Losungen Von Natriumalkylsulfaten Gegen N-Heptan. Angew Chem-Int Edit 69: 537-537

61. Dahanayake M, Cohen AW and Rosen MJ (1986) Relationship of Structure to Properties of Surfactants .13. Surface and Thermodynamic Properties of Some Oxyethylenated Sulfates and Sulfonates. J Phy Chem 90: 2413-2418

62. Rosen MJ, Zhu YP and Morrall SW (1996) Effect of Hard River Water on the Surface Properties of Surfactants. J Chem Eng Data 41: 1160-1167

63. Venable RL and Nauman RV (1964) Micellar Weights of + Solubilization of Benzene by Series of Tetradecylammonium Bromides . Effect of Size of Charged Head. J Phy Chem 68: 3498-&

64. Rosen MJ, Dahanayake M and Cohen AW (1982) Relationship of Structure to Properties in Surfactants .11. Surface and Thermodynamic Properties of N-Dodecylpyridinium Bromide and Chloride. Colloids Surf 5: 159-172

65. Sierra ML and Svensson M (1999) Mixed Micelles Containing Alkylglycosides: Effect of the Chain Length and the Polar Head Group. Langmuir 15: 2301-2306

66. Joshi T, Mata J and Bahadur P (2005) Micellization and Interaction of Anionic and Nonionic Mixed Surfactant Systems in Water. Colloid Surf A-Physicochem Eng Asp 260: 209-215

67. Prokhorova GV and Glukhareva NA (2011) Micellization in Aqueous Solutions of Mixed Surfactants Containing Alkylpolyglucosides. Colloid J 73: 841-845

68. Hoffmann H and Possnecker G (1994) The Mixing Behavior of Surfactants. Langmuir 10: 381-389

69. Sood AK, Singh K and Banipal TS (2010) Study of Micellization Behavior of Some Alkyldimethylbenzyl Ammonium Chloride Surfactants in the Presence of Polymers. J Dispersion Sci Technol 31: 62-71

70. Ekwall P and Mylius W (1929) Acidic Sodium Salts of Lauric Acid. Berichte Der Deutschen Chemischen Gesellschaft 62: 2687-2690

71. Ekwall P and Mylius W (1929) On Acid Sodium Salts of Palmitic Acid. Berichte Der Deutschen Chemischen Gesellschaft 62: 1080-1084

72. Ekwall P (1933) System of Palmitin Acid-Sodium Palmitate. Z Anorg Allg Chem 210: 337-349

73. Ekwall P and Lindblad LG (1941) Information on the Constitution of Diluted Soap Solutions Iv the Hydroxyl Ion Activity of Sodium Solutions at 20 Degrees. Kolloid-Z 94: 42-57

74. McBain JW and Field MC (1933) Phase Rule Equilibria of Acid Soaps. I Anhydrous Acid Potassium Laurate. J Phys Chem 37: 675-684

75. McBain JW and Field MC (1933) Phase-Rule Equilibria of Acid Soaps Part Ii Anhydrous Acid Sodium Palmitates. Journal of the Chemical Society 920-924

76. Lynch ML, Pan Y and Laughlin RG (1996) Spectroscopic and Thermal Characterization of 1:2 Sodium Soap Fatty Acid Acid-Soap Crystals. J Phys Chem 100: 357-361

77. Lynch ML (1997) Acid-Soaps. Curr Opin Colloid Interface Sci 2: 495-500

78. Wen XY, Lauterbach J and Franses EI (2000) Surface Densities of Adsorbed Layers of Aqueous Sodium Myristate Inferred from Surface Tension and Infrared Reflection Absorption Spectroscopy. Langmuir 16: 6987-6994

79. Kanicky JR and Shah DO (2003) Effect of Premicellar Aggregation on the Pk(a) of Fatty Acid Soap Solutions. Langmuir 19: 2034-2038

80. Saitta AM and Klein ML (2003) Proton Tunneling in Fatty Acid/Soap Crystals? J Chem Phys 118: 1-3

81. Heppenstall-Butler M and Butler MF (2003) Nonequilibrium Behavior in the Three-Component System Stearic Acid-Sodium Stearate-Water. Langmuir 19: 10061-10072

82. Zhu S, Heppenstall-Butler M, Butler MF, Pudney PDA, Ferdinando D and Mutch KJ (2005) Acid Soap and Phase Behavior of Stearic Acid and Triethanolamine Stearate. J Phys Chem B 109: 11753-11761

83. Fernandez-Leyes MD, Schulz PC and Messina PV (2008) Ph and Surface Tension Dependence of Mixed Sodium Deoxycholate-Sodium Dehydrocholate Pre-Micellar Aggregation in Aqueous Solution. Colloid Surf A-Physicochem Eng Asp 329: 24-30

84. Mysels KJ (1986) Surface-Tension of Solutions of Pure Sodium Dodecyl-Sulfate. Langmuir 2: 423-428

85. Lucassen J (1966) Hydrolysis and Precipitates in Carboxylate Soap Solutions. J Phys Chem 70: 1824-&

86. Frumkin A (1925) The Capillary Curve of Higher Fatty Acids and the Constitutive Equation of the Surface Layer. Zeit Fur Phy Chem--Stoch Und Ver 116: 466-484

87. Kling W and Lange H (1957) Grenzflachenspannung Wassriger Losungen Von Natriumalkylsulfaten Gegen N-Heptan. Angew Chem-Int Edit 69: 537-537

88. Rosen MJ, Zhu YP and Morrall SW (1996) Effect of Hard River Water on the Surface Properties of Surfactants. J Chem Eng Data 41: 1160-1167

89. Venable RL and Nauman RV (1964) Micellar Weights of + Solubilization of Benzene by Series of Tetradecylammonium Bromides . Effect of Size of Charged Head. J Phys Chem 68: 3498-&

90. Rosen MJ, Dahanayake M and Cohen AW (1982) Relationship of Structure to Properties in Surfactants .11. Surface and Thermodynamic Properties of N-Dodecylpyridinium Bromide and Chloride. Colloids and Surfaces 5: 159-172

91. Cistola DP, Hamilton JA, Jackson D and Small DM (1988) Ionization and Phase-Behavior of Fatty-Acids in Water - Application of the Gibbs Phase Rule. Biochemistry 27: 1881-1888

92. Kanicky JR, Poniatowski AF, Mehta NR and Shah DO (2000) Cooperativity among Molecules at Interfaces in Relation to Various Technological Processes: Effect of Chain Length on the Pk(a) of Fatty Acid Salt Solutions. Langmuir 16: 172-177

93. Decastro FHB and Borrego AG (1995) Modification of Surface-Tension in Aqueous-Solutions of Sodium Oleate According to Temperature and Ph in the Flotation Bath. Journal of Colloid and Interface Science 173: 8-15

94. Pugh R and Stenius P (1985) Solution Chemistry Studies and Flotation Behavior of Apatite, Calcite and Fluorite Minerals with Sodium Oleate Collector. Int J Miner Process 15: 193-218

95. Cui XH, Jiang Y, Yang CS, Lu XY, Chen H, Mao SZ, Liu ML, Yuan HZ, Luo PY and Du YR (2010) Mechanism of the Mixed Surfactant Micelle Formation. J Phys Chem B 114: 7808-7816

96. Wang T-Z, Mao S-Z, Miao X-J, Zhao S, Yu J-Y and Du Y-R (2001) 1h Nmr Study of Mixed Micellization of Sodium Dodecyl Sulfate and Triton X-100. Journal of Colloid and Interface Science 241: 465-468

97. Nilsson PG, Wennerstrom H and Lindman B (1983) Structure of Micellar Solutions of Non-Ionic Surfactants - Nuclear Magnetic-Resonance Self-Diffusion and Proton Relaxation Studies of Poly(Ethylene Oxide) Alkyl Ethers. J Phys Chem 87: 1377-1385

98. Liu J, Jiang Y, Chen H, Mao SZ, Du YR and Liu ML (2012) Probing Dynamics and Mechanism of Exchange Process of Quaternary Ammonium Dimeric Surfactants, 14-S-14, in the Presence of Conventional Surfactants. J Phys Chem B 116: 14859-14868

99. Zhao J and Fung BM (1993) Nmr-Study of the Transformation of Sodium Dodecyl-Sulfate Micelles. Langmuir 9: 1228-1231

100. Rabi, II, Zacharias JR, Millman S and Kusch P (1938) A New Method of Measuring Nuclear Magnetic Moment. Phys Rev 53: 318-318

101. Crews P (1998) Organic Structure Analysis. Topics in Organic Chemistry